

การใช้ตะแกรงโลหะเพื่อเพิ่มประสิทธิภาพการดูดซึมสารอินทรีย์ไอระเหยในช่องขนาดไมโคร



บทคัดย่อและแฟ้มข้อมูลฉบับเต็มของวิทยานิพนธ์ตั้งแต่ปีการศึกษา 2554 ที่ให้บริการในคลังปัญญาจุฬาฯ (CUIR)
เป็นแฟ้มข้อมูลของนิสิตเจ้าของวิทยานิพนธ์ ที่ส่งผ่านทางบัณฑิตวิทยาลัย

The abstract and full text of theses from the academic year 2011 in Chulalongkorn University Intellectual Repository (CUIR)
are the thesis authors' files submitted through the University Graduate School.

วิทยานิพนธ์นี้เป็นส่วนหนึ่งของการศึกษาตามหลักสูตรปริญญาวิศวกรรมศาสตรมหาบัณฑิต
สาขาวิชาวิศวกรรมเคมี ภาควิชาวิศวกรรมเคมี
คณะวิศวกรรมศาสตร์ จุฬาลงกรณ์มหาวิทยาลัย
ปีการศึกษา 2559
ลิขสิทธิ์ของจุฬาลงกรณ์มหาวิทยาลัย

USE OF METAL MESH TO INCREASE ABSORPTION EFFICIENCY OF VOLATILE ORGANIC
COMPOUND IN MICROCHANNEL

Mr. Rachata Prasomsup



A Thesis Submitted in Partial Fulfillment of the Requirements
for the Degree of Master of Engineering Program in Chemical Engineering

Department of Chemical Engineering

Faculty of Engineering

Chulalongkorn University

Academic Year 2016

Copyright of Chulalongkorn University

Thesis Title	USE OF METAL MESH TO INCREASE ABSORPTION EFFICIENCY OF VOLATILE ORGANIC COMPOUND IN MICROCHANNEL
By	Mr. Rachata Prasomsup
Field of Study	Chemical Engineering
Thesis Advisor	Associate Professor Varong Pavarajarn, Ph.D.

Accepted by the Faculty of Engineering, Chulalongkorn University in Partial Fulfillment of the Requirements for the Master's Degree

.....Dean of the Faculty of Engineering
(Associate Professor Supot Teachavorasinskun, Ph.D.)

THESIS COMMITTEE

.....Chairman
(Assistant Professor Apinan Soottitantawat, D.Eng.)

.....Thesis Advisor
(Associate Professor Varong Pavarajarn, Ph.D.)

.....Examiner
(Paravee Vas-Umnuay, Ph.D.)

.....External Examiner
(Busarakam Charnhattakorn, Ph.D.)

รชตะ ประสมทรัพย์ : การใช้ตะแกรงโลหะเพื่อเพิ่มประสิทธิภาพการดูดซึมสารอินทรีย์ไอระเหยในช่องขนาดไมโคร (USE OF METAL MESH TO INCREASE ABSORPTION EFFICIENCY OF VOLATILE ORGANIC COMPOUND IN MICROCHANNEL) อ.ที่ปรึกษาวิทยานิพนธ์หลัก: รศ. ดร.วรงค์ ปวรจารย์, 85 หน้า.

การปล่อยสารอินทรีย์ไอระเหยสามารถทำให้เกิดปัญหาทางด้านสิ่งแวดล้อมและสุขภาพ วิธีการดูดซึมเป็นวิธีการหนึ่งที่มีประสิทธิภาพในการลดปริมาณการปล่อยสารอินทรีย์ไอระเหยเนื่องจากวิธีการนี้มีความจุที่สูงและมีต้นทุนการดำเนินงานต่ำ ในงานวิจัยนี้ได้มีการใช้ช่องขนาดไมโครเพื่อเพิ่มการถ่ายโอนมวลสารและเพิ่มพื้นที่ผิวสัมผัสจำเพาะระหว่างแก๊สและตัวทำละลายของเหลว นอกจากนี้ตะแกรงสแตนเลสถูกนำมาปรับใช้เพื่อป้องกันไม่ให้แก๊สและตัวทำละลายของเหลวกระจายจากภูมิภาคหนึ่งไปยังอีกภูมิภาคหนึ่ง โดยตะแกรงสแตนเลสถูกวางไว้ระหว่างช่องการไหลของแก๊สและตัวทำละลายของเหลว ขนาดของตะแกรง สแตนเลสได้ถูกปรับเปลี่ยนโดยใช้ตะแกรงสแตนเลสเลขที่ 100, 200 และ 300 โทลูอินถูกใช้เป็นตัวแทนของสารอินทรีย์ไอระเหยและน้ำมันพืชถูกใช้เป็นตัวทำละลายของเหลว จากผลของการศึกษาพบว่าอัตราส่วนของอัตราการไหลของแก๊สต่อตัวทำละลายของเหลวเป็นตัวควบคุมการแยกของแก๊สออกจากตัวทำละลายของเหลว อีกทั้งยังพบว่าขนาดและสมบัติของพื้นผิวของตะแกรงสแตนเลสมีบทบาทสำคัญในการรักษาให้แก๊สและตัวทำละลายของเหลวแยกออกจากกัน นอกจากนี้ประสิทธิภาพการกำจัดโทลูอินขึ้นอยู่กับอิทธิพลของอัตราการไหลของแก๊ส อัตราการไหลของตัวทำละลายของเหลว ความยาวของช่อง ความหนาของช่อง ขนาดของรู ตะแกรงและความเข้มข้นของแก๊สขาเข้า ประสิทธิภาพการกำจัดโทลูอินในช่องขนาดไมโครในงานวิจัยนี้ยังสูงถึงร้อยละ 97 และสุดท้ายสัมประสิทธิ์การถ่ายโอนมวลสารอิงจากปริมาตรด้านของเหลวในงานวิจัยนี้ได้ถูกคำนวณและพบว่ามีค่าสูงถึง 0.00165 ต่อวินาที

ภาควิชา วิศวกรรมเคมี

ลายมือชื่อนิสิต

สาขาวิชา วิศวกรรมเคมี

ลายมือชื่อ อ.ที่ปรึกษาหลัก

ปีการศึกษา 2559

5870227821 : MAJOR CHEMICAL ENGINEERING

KEYWORDS: VOC / ABSORPTION / MICROCHANNEL / MESH

RACHATA PRASOMSUP: USE OF METAL MESH TO INCREASE ABSORPTION EFFICIENCY OF VOLATILE ORGANIC COMPOUND IN MICROCHANNEL. ADVISOR: ASSOC. PROF. VARONG PAVARAJARN, Ph.D., 85 pp.

Volatile organic compounds (VOCs) emissions can cause environmental problems and public health. Absorption is an effective method to reduce VOCs emission because it provides high capacity and low operating costs. In this work, microchannel was applied to increase mass transfer and interfacial area between the gas and liquid solvent. Moreover, a stainless steel mesh was used to prevent dispersion of one phase into the other. The stainless steel mesh was placed between two channels gas- and liquid-sides of the channel. The stainless steel mesh size was varied by using stainless steel mesh number 100, 200, and 300. Toluene was used as a representative of VOC and vegetable oil was used as a liquid solvent. The result of this work was found that the gas to liquid solvent flow rate ratio was a factor to control separation of gas and the liquid solvent. Moreover, size and surface property of stainless steel mesh played a crucial role in keeping gas and the liquid solvent separated. In addition, the removal efficiency of toluene depended on the influence of gas flow rate, liquid flow rate, channel length, channel thickness, mesh size and inlet gas concentration. Moreover, the removal efficiency of toluene was up to 97 % in this work. Finally, the liquid-side volumetric mass transfer coefficients in this work were calculated and found to be as high as 0.00165 s^{-1} .

Department: Chemical Engineering Student's Signature

Field of Study: Chemical Engineering Advisor's Signature

Academic Year: 2016

ACKNOWLEDGEMENTS

First of all, I would like to convey my sincere thanks to my advisor, Associate Professor Varong Pavarajarn, for having introduced this project which improves me to acquire more experience and knowledge. His advice and encouraging words keep me moving forward.

Moreover, I also would like to express my grateful thanks to my thesis examiners, Assistant Professor Apinan Soottitantawat, Dr. Paravee Vasumnuay and Dr. Busarakam Charnhattakorn, for their recommendation.

For all members of Center of Excellence in Particle Technology, I really appreciate their help, advice and friendship which support me to achieve this goal. Especially people at the Themo building, I am thankful for everything you have done.

Finally, I would like to express my gratitude to my family for their support and love. Thank you for giving me an opportunity to do the thing that I thought I cannot do it. Without their encouragement, this achievement would not have been possible.

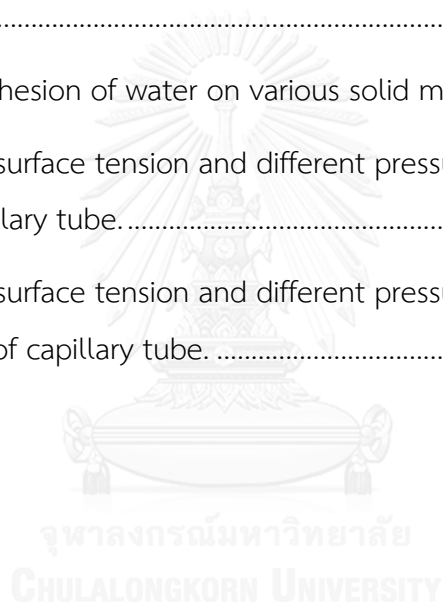
CONTENTS

	Page
THAI ABSTRACT	iv
ENGLISH ABSTRACT	v
ACKNOWLEDGEMENTS	vi
CONTENTS.....	vii
LIST OF TABLES	ix
LIST OF FIGURES.....	x
CHAPTER I INTRODUCTION.....	1
1.1 Objective	3
1.2 Scopes of work.	3
CHAPTER II FUNDAMENTAL THEORY AND LITERATURE REVIEWS.....	4
2.1 Volatile organic compounds (VOCs)	4
2.2 Volatile organic compounds removal methods.....	6
2.3 Gas absorption	10
2.4 Solubility of VOCs in liquid solvent.....	13
2.5 Microchannel.....	14
2.6 Mesh contactor.....	16
2.7 Pressure drop in microchannel.....	21
2.8 Literature reviews.....	24
CHAPTER III EXPERIMENTAL	27
3.1 Chemicals.....	27
3.2 Microchannel apparatus	27
3.3 Experimental setup and procedures	28

	Page
3.4 Analytical instrument	29
CHAPTER IV RESULTS AND DISCUSSION.....	31
4.1 Henry's law constant	31
4.2 Flow pattern regime	34
4.3 Capillary action	40
4.4 Pressure drop in microchannel.....	50
4.5 Absorption.....	52
CHAPTER V CONCLUSION.....	68
5.1 Summary of the results	68
5.2 Conclusion	69
REFERENCES.....	71
APPENDIX	73
APPENDIX A Calibration curve of toluene	73
APPENDIX B Calculation	74
VITA	85

LIST OF TABLES

Table 2.1 Some of common volatile organic compounds	4
Table 2.2 Various methods for reducing volatile organic compounds	10
Table 2.3 Henry' law constant of toluene in various liquid solvent.....	14
Table 2.4 the comparison of mass transfer coefficients and interfacial area achieved using present micro scale reactors with conventional gas-liquid absorption system.	15
Table 2.5 Work of adhesion of water on various solid materials	18
Table 4.1 The level, surface tension and different pressure of water within different type of capillary tube.....	42
Table 4.2 The level, surface tension and different pressure of vegetable oil within different type of capillary tube.	44



LIST OF FIGURES

Figure 2.1 Classification of volatile organic compounds removal method.....	6
Figure 2.2 Structure of sunflower oil.....	12
Figure 2.3 Scheme of dispersion in microchannel.....	15
Figure 2.4 Scheme of a mesh contactor.....	16
Figure 2.5 Illustration of a capillary force within narrow pore.....	17
Figure 2.6 Mass transfer regions in mesh contactor.....	19
Figure 2.7 Scheme of momentum balance in gas and liquid channel.....	21
Figure 2.8 Scheme of the boundary conditions of the rectangular cross-section channel.....	23
Figure 3.1 Scheme of the microchannel.....	28
Figure 3.2 Scheme of the experimental setup.....	29
Figure 3.3 Shimadzu 14B gas chromatograph.....	30
Figure 4.1 Equilibrium curve of toluene concentration in vapor – liquid equilibrium.....	32
Figure 4.2 Concentrations of toluene and vegetable oil in vapor-liquid equilibrium.....	33
Figure 4.3 Flow pattern regime between gas and vegetable oil using mesh number 50.....	35
Figure 4.4 Flow pattern regime between gas and vegetable oil using mesh number 100.....	36
Figure 4.5 Flow pattern regime between gas and vegetable oil using mesh number 200.....	38

Figure 4.6 Flow pattern regime between gas and vegetable oil using mesh number 300.....	39
Figure 4.7 Capillary action of water within hydrophobic capillary tube and glass capillary tube.....	41
Figure 4.8 Capillary action of vegetable oil within hydrophobic capillary tube and glass capillary tube.....	43
Figure 4.9 Hydrophobic stainless steel mesh and hydrophilic stainless steel mesh	45
Figure 4.10 Flow pattern regime between gas and vegetable oil using hydrophobic mesh number 100	46
Figure 4.11 Effect of mesh size on the different pressure of vegetable oil.....	47
Figure 4.12 Flow pattern regime between gas and water using stainless steel mesh number 100	48
Figure 4.13 Comparison of Different pressure within stainless steel mesh number 100 between vegetable oil and water	49
Figure 4.14 Pressure drop in gas channel	50
Figure 4.15 Pressure drop in liquid channel	51
Figure 4.16 Effect of gas flow rate on toluene removal efficiency	53
Figure 4.17 Effect of gas flow rate on the liquid-side volumetric mass transfer coefficients	54
Figure 4.18 Effect of liquid flow rate on toluene removal efficiency.....	56
Figure 4.19 Effect of liquid flow rate on the liquid-side volumetric mass transfer coefficients	57
Figure 4.20 Effect of liquid flow rate on toluene removal efficiency by using 6 centimeters microchannel.....	58

Figure 4.21 Effect of liquid flow rate on the liquid-side volumetric mass transfer coefficients by using 6 centimeters microchannel.....	60
Figure 4.22 Effect of mesh size on toluene removal efficiency.....	61
Figure 4.23 Effect of mesh size the liquid-side volumetric mass transfer coefficients	62
Figure 4.24 Effect of mesh size on toluene removal efficiency.....	63
Figure 4.25 Effect of channel thickness the liquid-side volumetric mass transfer coefficients	64
Figure 4.26 Effect of inlet gas concentration on the toluene removal efficiency.	65
Figure 4.27 Effect of inlet gas concentration the liquid-side volumetric mass transfer coefficients	66
Figure 4.28 Effect of modified stainless steel mesh on the toluene removal efficiency	67

CHAPTER I

INTRODUCTION

In the present, air pollution is the most serious issue because it can cause damage to human, animals, plants, and water. Many Industries such as chemical, petrochemical, and pharmaceutical industry are considered that they are sources of emission of toxic gasses. One of toxic gas is volatile organic compounds (VOCs) which have a high vapor pressure at ambient temperature and atmosphere. Because of their properties, volatile organic compounds affect the growth of plants and the health of human and animals in the short and long term. However, volatile organic compounds from industry emission are treated ineffectively. So, the emissions of volatile organic compounds from industry are concerned that it can cause environmental problems and public health. In order to reduce the volatile organic compounds emissions, various methods are available to reduce volatile organic compounds such as thermal or catalytic oxidations, adsorption, condensation, absorption, membrane permeation and biological treatments [1].

Absorption process is an effective method to reduce volatile organic compounds emission from industry by using a liquid solvent because it provides a high surface area, high capacity, and low operating costs. The selection of the liquid solvent for absorption depends on the volatile organic compounds solubility in the liquid solvent. In addition, the liquid solvent should have very good chemical and thermal stability, low volatility, low toxicity and high boiling point [2, 3]. Vegetable oil is an alternative solvent which has low price and suitable properties to reduce volatile organic compounds emission. Besides, vegetable oil is non-polar compounds which may absorb volatile organic compounds easily.

Generally, volatile organic compounds are absorbed in a large equipment such as a packed column, stripping column and bubble column which have low interfacial area, surface area per volume ratio, and low mass transfer between gas and liquid

solvent. A microchannel is an alternative technique for reducing mass transfer resistances between gas phase and liquid solvent because it has short diffusion distance between gas and liquid solvent. Due to their small internal dimensions, the microchannel provides a high interfacial area between gas and liquid phase. In addition, microchannel has several advantages rather than a large equipments such as short residence time, and safety. However, when gas directly contacts with a liquid solvent, gas may break liquid to be unstable. Consequently, the operating interfacial area is lower than the available interfacial area [4]. So, stainless steel mesh is applied to allow gas and liquid solvent contact without dispersion of one phase into the other.

Moreover, the capillary force within two types of stainless steel mesh pores is studied because the capillary force depends on the adhesion force which relies on the property of liquid solvent and solid pores. Therefore, the capillary force within stainless steel mesh pores is supposed that it is a significant factor to separate gas and the liquid solvent.

Many research has been investigated the absorption of volatile organic compounds in a microchannel for increasing the removal efficiency such as falling film microchannel, circular cross-sectional microchannel, and silicon nitride mesh contactor microchannel. The most research studied the absorption of volatile organic compounds when gas dispersed into the liquid solvent. There has a few research which studies the absorption when gas and liquid solvent are separated like membrane gas absorption but the stainless steel mesh which has high contact area was not studied. Besides, the effect of the different property of mesh on the absorption and mass transfer coefficient are not studied.

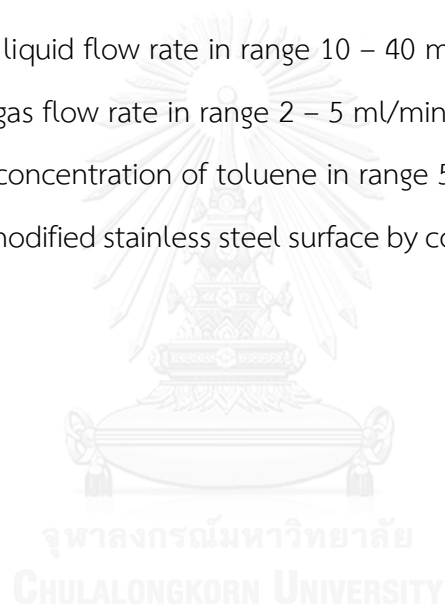
This work studies the absorption process of volatile organic compound by using stainless steel mesh in a microchannel. The stainless steel mesh is placed between two channels, gas, and liquid channel, to protect breaking of liquid by gas. In this work, toluene is used as a representative of the volatile organic compound while vegetable oil is used as a representative of a liquid solvent.

1.1 Objective

The objective of this work is to study the using of metal mesh to increase absorption efficiency of toluene/air mixture gas by using vegetable oil as a liquid solvent in a microchannel.

1.2 Scopes of work.

- Study the effect of mesh size in a microchannel by using mesh number 100, 200, and 300.
- Study the effect of liquid flow rate in range 10 – 40 ml/h.
- Study the effect of gas flow rate in range 2 – 5 ml/min.
- Study the effect of concentration of toluene in range 5,000 – 25,000 ppm.
- Study the effect of modified stainless steel surface by coating hydrophobic substance.



CHAPTER II

FUNDAMENTAL THEORY AND LITERATURE REVIEWS

2.1 Volatile organic compounds (VOCs)

Volatile organic compounds are chemical compounds which have vapor pressure more than 1 mmHg at ambient temperature. This property results from a low boiling point a trait known as volatility and it can easily vaporize into the surrounding air. Sometimes, the volatile organic compounds are defined and classified by their boiling point. The molecule of volatile organic compounds mainly contains carbon and, hydrogen and other molecule such as oxygen, nitrogen, sulfur, and halogens. Table 2.1 shows some of the common volatile organic compounds.

Table 2.1 Some of common volatile organic compounds [5]

Serial Number	Volatile Organic Compounds
1	Acetaldehyde
2	Acetone
3	Benzene
4	Carbon tetrachloride
5	Ethyl acetate
6	Ethylene glycol
7	Formaldehyde
8	Heptane
9	Hexane
10	Isopropyl alcohol
11	Methyl ethyl ketone
12	Methyl chloride
13	Monomethyl ether
14	Naphthalene
15	Styrene
16	Toluene
17	Xylene

There are many sources of emission of volatile organic compounds such as food industry, agriculture, electronic industry, chemical industry, pharmaceutical industry, wastewater treatment, painting or coating manufacturer, petrochemical processes, and highway construction.

2.1.1 Environmental effects of volatile organic compounds

The volatile organic compounds emissions from many industries as we describe above are a significant factor in the creation of environmental problems. Volatile organic compounds are involved in photochemical reactions which react with nitrogen oxides in the atmosphere to form ozone and entail environmental hazards such as global warming, acid rain and air – borne toxics [6]. Ozone in the stratosphere is helpful because it helps to protect the sun's ultraviolet radiation but ozone which is produced by volatile organic compounds inhibits the troposphere. Troposphere (ground – level) ozone is harmful because it is the formation of smog. Thus, high troposphere ozone levels can damage to the growth of plants and crop yields.

2.1.2 Health effects of volatile organic compounds

The volatile organic compounds have an influence on human health. Because of increasing of volatile organic compounds, the troposphere ozone on the ground increases as well. The increasing of troposphere ozone will be dangerous to people who live on the ground because excess amounts of ozone can affect their health. Troposphere ozone can cause permanent damage to a lung tissue, liver, kidney, nervous system, and immune system. Moreover, a person who acquires volatile organic compounds in the short term will have a headache, dizziness, and respiratory irritation.

2.2 Volatile organic compounds removal methods

Various methods are available for reducing the emission of volatile organic compounds. The volatile organic compounds removal methods can be classified into two main groups: process and equipment modification method and add-on control method as shown in Figure 2.1. Process and equipment modification method is a modification of the process equipment, raw material or changing in operating conditions. Add-on control method can be classified into two types: destruction and recovery method. In the destruction method, volatile organic compounds are destroyed by oxidation or bacteria. Another method is recovery method which volatile organic compounds are not destroyed [5].

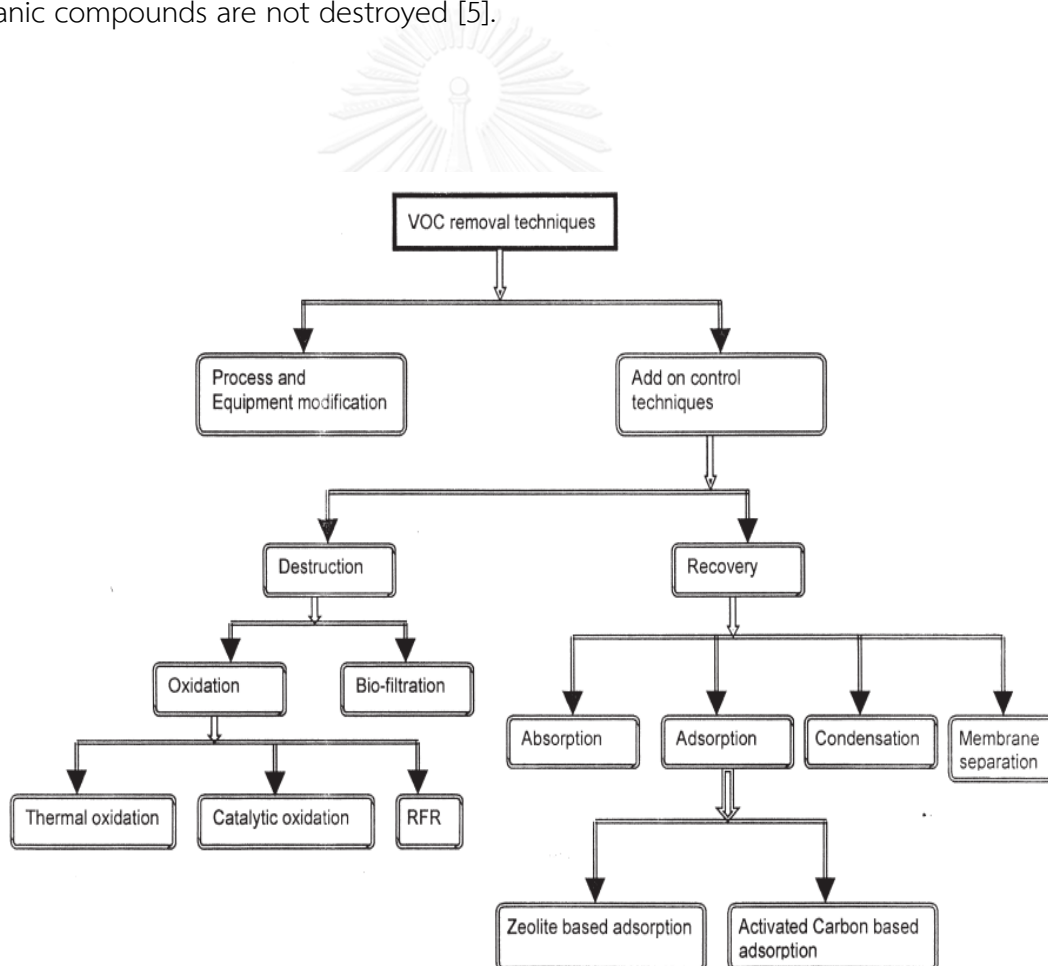


Figure 2.1 Classification of volatile organic compounds removal method

2.2.1 Thermal oxidation

Thermal oxidation method is a system that combust volatile organic compounds at 1,300 – 1800°F of temperature. This method is designed to handle a capacity of 1,000 – 500,000 cubic feet per minute (cfm) and it is available for a range of volatile organic compounds concentration from 100 to 2,000 ppm. The volatile organic compounds which are difficult to combust need to require greater heat and retention time to combust volatile organic compounds completely. However, the thermal oxidation method can produce high levels of nitrogen oxide which is a pollutant in the air. Moreover, the volatile organic compounds which have halogenated molecule can convert to be an acid which can corrode the materials. So, this method needs a further treatment such as scrubbers.

2.2.2 Catalyst oxidation

Catalyst oxidation method is similar to thermal oxidation method that volatile organic compounds are combusted directly. This method, the catalyst can reduce the energy requirement of combustion. So, the operating condition is lower than thermal oxidation condition. The operating condition is about 700 – 900°F. Catalyst oxidation is designed to handle a capacity of 1,000 – 100,000 cfm and it is available for a range of volatile organic compounds concentration from 100 to 2,000 ppm. However, the catalyst oxidation in large scale is not popular as thermal oxidation because the high costs of catalyst loading. In addition, the catalyst oxidation method can produce a pollutant like thermal oxidation which needs a proper treatment. Catalysts which are used in this process are sensitive with sulphur, silicon and chloride.

2.2.3 Bio-filtration

The bio-filtration method depends on the ability of micro-organisms to convert volatile organic compounds under aerobic conditions. The products from this method contain carbon dioxide, water, inorganic products, and biomass. The temperature of operating condition is about 50 – 105°F. Bio-filtration is designed to handle a capacity lower than 14,000 cfm and it is available for a range of volatile organic compounds

concentration lower than 5,000 ppm. This method has many advantages such as mild operating condition, less pollutant, less initial investment, and non-hazardous. However, this method is slow and the material cannot recover.

2.2.4 Condensation

The condensation method produces a liquid product of volatile organic compounds from the gas stream. This method is most efficient for volatile organic compounds which have boiling points above 100°F and high concentrations above 5,000 ppm. The low boiling point volatile organic compounds need to require greater cooling which needs more operating costs. The liquid from this method can be reused in the process. For example, using a liquid of volatile organic compounds as a solvent to clean the equipment, or using a liquid of volatile organic compounds as a boiler fuel.

2.2.5 Membrane-based gas absorption

The membrane-based gas absorption (MGA) process is based on a gas and liquid phase contact across the hydrophobic microporous membrane. The membrane is used as a physical barrier between gas and liquid phase. This method is used only on the laboratory scale and pilot plants. There are many advantages of using membrane absorption such as high removal efficiency of volatile organic compounds, low operating costs, and no further treatment. Moreover, the membrane bases gas absorption process can protect the flooding problem [7]. However, membranes are rare and expensive.

2.2.6 Adsorption

The adsorption process involves the interaction between adsorbate and adsorbent by the weak Van der Waals force of attraction. In this process, the volatile organic compounds are attracted on the surface and in the pores of the adsorbent. The selection of the adsorbent depends on the application. The adsorbent must have a large specific surface area such as activated carbon or zeolite. This process is designed to handle a low capacity of 100 – 6,000 cfm and it is available for a range of volatile organic compounds concentration from 700 to 10,000 ppm. This method has good removal efficiency but it requires a high capital investment and operating costs.

2.2.7 Absorption

Absorption process is an effective method to remove volatile organic compounds from a gas stream. It is a physical process that contacts the contaminated gas with a liquid solvent. This process is designed to handle a low capacity of 2,000 – 100,000 cfm and it is available for a range of volatile organic compounds concentration from 500 to 15,000 ppm. Absorption process has many advantages such as simple process, good efficiency, high capacity, high surface area, low investment and using with a wide range of concentrations.

Table 2.2 shows the various methods for reducing volatile organic compounds. It shows that absorption method is proper with the removal volatile organic compound process which has high capacity and wide range concentration of volatile organic compounds.

Table 2.2 Various methods for reducing volatile organic compounds [5]

Techniques	VOC content (ppm)	Moisture content	Capacity range (cfm)	Temperature (°F)	Special remarks
Thermal oxidation	Greater than 20 but less than 25% of LEL	Normal 10–40% RM	1000–500,000	700	Requires elaborate safety measures
Catalytic oxidation	100–1000 but always less than 25% of LEL	Normal 10–40% RM	1000–10,000	300	An elaborate safety measure
Bio-filtration	<5000	>90%	<14,000	50–105	Precaution that VOC should not be toxic to microbes
Condensation	5000–10,000	20–80%	100–20,000	Ambient	–
Absorption	500–15,000	Normal	2000–100,000	Normal	Stripping should be easily possible
Adsorption					
Activated carbon	700–10,000 (but always less than 25% of LEL)	<50%	100–6000	<130	Must be desorbed from another adsorbent
Zeolite	1000–10,000 (but always less than 25% of LEL)	~94–96%	100–6000	ambient	Must be desorbed from another adsorbent
Membrane separation	Very low concentration to 25% of LEL	90–99%	200–1500	ambient	No further operation is required

2.3 Gas absorption

Gas absorption is a process that involves in the diffusion between the components in a gas stream and liquid solvent. The components in gas stream are removed by contact with a liquid solvent for the purposes of preferentially dissolving one or more components of the gas and to provide the solution of them in the liquid. This process has many variables which are a significant role in absorption efficiency as follows.

- Absorbent or liquid solvent
- Concentration of gas mixture
- Carrier gas
- Surface area between gas and liquid solvent
- Solubility of gas in liquid solvent
- Flow rate of gas and liquid solvent

Moreover, the removal efficiency of volatile organic compounds depends on pressure drop. However, the packing type of packed absorption is not a significant role for reducing volatile organic compounds [8].

2.3.1 The selection of liquid solvent for gas absorption [9]

There have a lot of solvents to remove some constituent from gas. The following properties are important considerations:

1. Gas solubility: The solubility should be high. The solvents of a chemical nature similar to that of the solute to be absorbed will provide good solubility. For example, the hydrocarbon oils are used to remove organic compounds from gas.

2. Volatility: The liquid solvent should have a low vapor pressure since the gas leaving an absorption operation is ordinarily saturated with the solvent and much may thereby be lost.

3. Corrosiveness: The liquid solvent should not erode materials of construction.

4. Cost: The liquid solvent should be inexpensive and readily available.

5. Viscosity: Low viscosity of liquid solvent is preferred for reasons of rapid absorption rates, improving flooding, and low pressure drops on pumping.

Moreover, the liquid solvent should have proper properties such as high boiling point, easy to recover, and good chemical and thermal stability. Generally, the liquid solvents which use to absorb volatile organic compounds include water, mineral oils, or nonvolatile petroleum oils. The selection of the liquid solvent for absorption depends on the volatile organic compounds solubility in the liquid solvent. There have many liquid solvents which are usually used for remove volatile organic compounds such as polyethylene glycols, phthalates, adipates and silicone oil.

2.3.2 Using vegetable oil as a liquid solvent

Vegetable oil (sunflower oil) is very good for volatile organic compounds absorption because it has high temperature resistance, low viscosity, and making thermal regeneration possible. Moreover, it does not emit volatile organic compounds and it is cheap [6]. Sunflower oil consists with a monounsaturated and polyunsaturated fatty acid. It is mostly triglycerides with oleic acid and linoleic acid group of oils. The structure of sunflower oil is shown in Figure 2.2.

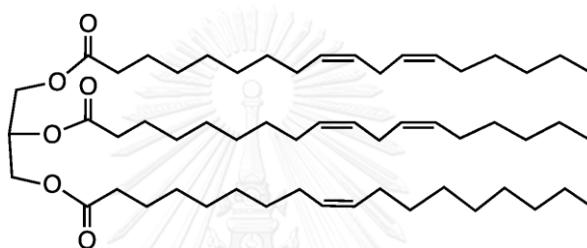


Figure 2.2 Structure of sunflower oil

From the structure of sunflower oil as shows above, it shows that sunflower oil is a non-polar compounds which can absorb volatile organic compounds easily. Moreover, it has a high monounsaturated fatty acids content which have a good absorption capacity with respect to volatile organic compound. Using fresh vegetable oil as an absorbent, toluene can be removed up to 95% which cannot be achieved in water [10].

2.4 Solubility of VOCs in liquid solvent

The VOCs gas can be absorbed by suitable liquid solvent because the different concentration of VOCs in gas phase and liquid solvent. The knowledge of VOCs gas solubility in liquid solvent is essential to describe the choosing of liquid solvent for the absorption of VOCs. The solubility of a gas in liquid solvent is observed that it is proportional to its partial pressure in gas phase and the equation which describes the solubility of a gas in liquid solvent is known as Henry's law [11]. Henry's law can be used to calculate the mole fraction of volatile organic compound which is dissolved in the liquid solvent. It is applied for low pressure by assuming that the vapor phase is an ideal gas. For volatile organic compound present as a very dilute solute in the liquid phase, Henry's law then states that the partial pressure of the species in the vapor phase is directly proportional to its liquid-phase mole fraction [12].

$$P_i = y_i P = H x_i \quad (2.1)$$

where H is a Henry's law constant, P_i is a partial pressure of component i in gas phase, y_i is the mole fraction of solute in the gas phase, x_i is the mole fraction of solute in the liquid phase and P is a total pressure.

The dimensionless Henry's law constant is defined by M.-D. Vuong, et. al. since the effect of the pressure on Henry's law constant is negligible at low pressure (less than 2 atm)[13].

$$H^* = \frac{C_{i,G}}{C_{i,L}} \quad (2.2)$$

where $C_{i,G}$ is an equilibrium gas concentration (mol/l) and $C_{i,L}$ is an equilibrium liquid concentration (mol/l).

The $1/H^*$ value of various liquid solvents are investigated by M.-D. Vuong, et. al. for choosing of the liquid solvent which absorbs VOCs in gas phase at 25°C and it

is shown in Table 2.3. The toluene is more soluble in liquid solvent which has high value of $1/H^*$ or low value of H^* .

Table 2.3 Henry' law constant of toluene in various liquid solvent [13]

Liquid solvent	$1/H^*$
DEHA	2821
n-Hexadecane	990
Oleyl alcohol	1637
PEG 400	1645
Water	4

2.5 Microchannel

Microchannel or microreactor is an interesting technique in the field of chemical engineer. Microchannel is a chemical apparatus with a small dimension less than one millimeter. It is suitable for multiphase processes such as gas absorption, hydrogenation, and liquid – liquid two phase extraction.

Moreover, using of the microchannel to environmental projects is an alternative way to enhance the removal efficiency of air pollution. Due to a small dimension, microchannel offers a high surface area to volume which enhances mass and heat transfer performance between gas and liquid phase while the pressure drop is at moderate levels. In addition, Microchannel has several advantages for reducing air pollution rather than a large equipment such as high interfacial area, short resident time, and safety [14].

The performance of microchannel is compared with the conventional absorption technology. The Table 2.4 reports the ranges of performance parameters

which is achieved in the present work and conventional absorbers. The range of mass transfer coefficient is wide because it depends on flow rate in each experiment.

Table 2.4 the comparison of mass transfer coefficients and interfacial area achieved using present micro scale reactors with conventional gas–liquid absorption system [15].

Type of system	$k_L (\times 10^{-5})$ (m/s)	a (m ² /m ³)	$k_L a (\times 10^{-2})$ (1/s)
Countercurrent packed columns	4–20	10–350	0.04–7
Co-current packed columns	4–60	10–1700	0.04–102
Bubble cap plate columns	10–50	100–400	1–20
Sieve plate columns	10–200	100–200	1–40
Bubble columns	10–40	50–600	0.5–24
Packed bubble columns	10–40	50–300	0.5–12
Horizontal and coiled tube reactors	10–100	100–2000	0.5–70
Vertical tube reactors	20–50	10–100	2–100
Spray columns	7–15	100–2000	0.07–1.5
Mechanically agitated bubble reactors	3–40	20–120	0.3–80
Submerged and plunging jet reactors	1.5–5	20–50	0.03–0.6
Hydro cyclone reactors	100–300	100–2000	2–15
Venturi reactors	50–100	160–2500	8–25
Microreactor	40–160	3400–9000	30–2100
Microreactor	231–2826	4000–4900	1100–13,200
Present study	893–2825	4000–14,941	3597–39,342

As describes above, microchannel is proper technique to improve the removal efficiency of volatile organic compounds. Due to the small channel, liquid fully flows within channel which gas can penetrate in liquid stream to form a slug of gas as shown in Figure 2.3. The liquid which is broken by gas causes a slug of gas which decreases the interfacial area [4]. So, mesh contactor is applied for improving this problem.

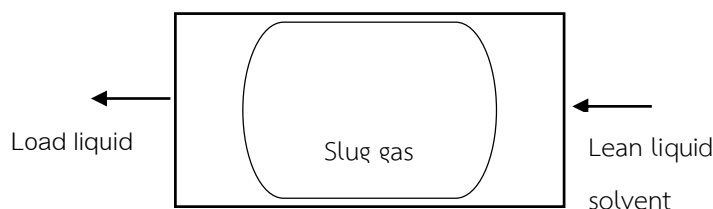


Figure 2.3 Scheme of dispersion in microchannel

2.6 Mesh contactor

Mesh contactor has many several advantages rather than membrane such as low mass transfer resistance, high porosity, good mechanical strength and well-ordered pore pattern [16]. The metal mesh is an alternative material which is cheap and easy available. The combination of microchannel technology and mesh contactor is a remarkable technique for reducing mass transfer resistance and protecting the dispersion of gas and liquid solvent at the same time. The sketch of a mesh for absorption process in the microchannel is shown in Figure 2.4.

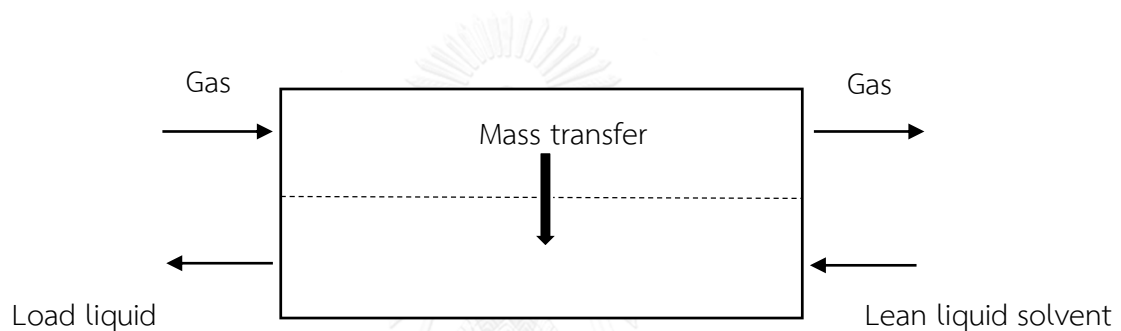


Figure 2.4 Scheme of a mesh contactor

The counter-current flow prepares the same different concentration of volatile organic compound between gas and liquid solvent at each position in the microchannel. The driving force in every position in the microchannel is quite constant which can remove volatile organic compound efficiently. In contrast, the co-current flow prepares a high different concentration of volatile organic compound between gas and liquid solvent at the inlet of the microchannel and the different concentration of volatile organic compound reduces along the length of the microchannel. It leads to high driving force at the inlet and low driving force at the outlet.

2.6.1 Capillary action within mesh pores

Capillary action within mesh pores can describe the flow pattern regime between a gas and liquid solvent. The capillary action within mesh pores is the result of cohesion force of liquid molecules and adhesion force of liquid molecules to the solid material to hold a liquid within pores as shown in Figure 2.5.

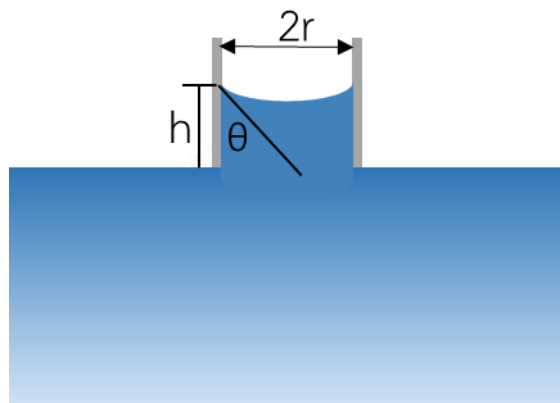


Figure 2.5 Illustration of a capillary force within narrow pore

The Young – Laplace equation can describe the capillary action within a narrow channel. It describes about the different pressure at interface between two static fluid like vegetable oil and air as following equation

$$\Delta P = \frac{2\gamma \cos\theta}{r} \quad (2.3)$$

where ΔP is a capillary pressure (N/m^2), γ is a liquid surface tension (N/m), r is a radius of pores (m) and θ is a contact angle (degree).

As the edges of the material are brought closer together, the interaction between liquid molecules and solid material is greater. The more narrow the pathway, small pore, lead to increasing of the surface tension and ratio of adhesion to cohesion.

Adhesion force is the tendency of two different surfaces that are attracted together. Generally, the several theories explain about adhesion which are based on surface-chemical phenomena such as adsorption, electrical theory, diffusion theory, and thermodynamic theory. The thermodynamic theory defines the adhesion as the reversible work per unit surface (W_a) to separate two phases that initially have a common interface [17]. W_a may be expressed as following equation

$$W_a = \gamma(\cos\theta + 1) \quad (2.4)$$

As the type of liquid and solid material are changed, the contact angle between liquid and solid material are changed. The contact angle depends on polarity of liquid and solid material. Table 2.5 shows the work of adhesion of water which has high polarity on the LDPE which has hydrophobic property and stainless steel and glass which have hydrophilic property.

Table 2.5 Work of adhesion of water on various solid materials

Solid materials	$W_{a_{\text{water}}}$
LDPE	6.2
Stainless steel	41.3
Glass	78

From Table 2.5, it shows that the properties of liquid and solid material may play a significant role on adhesion force which effect on the capillary force. So, the property of mesh is an influence of capillary force within mesh pores.

2.6.2 Mass transfer near the mesh contactor

The mass transfer of mesh contactor is determined by the consecutive steps in three phases including the diffusion of the component in gas phase from bulk gas to the gas-liquid interface within mesh pores, the dissolution of the component in gas phase into liquid solvent, and the diffusion of the component in liquid phase from the gas-liquid interface to the bulk liquid as shown in the Figure 2.6 [7].

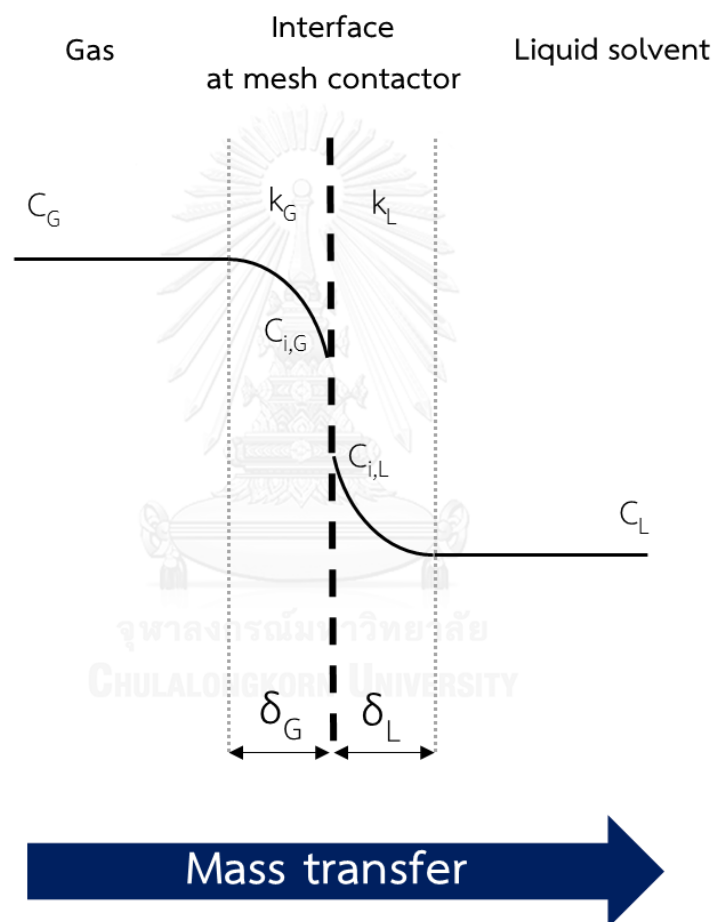


Figure 2.6 Mass transfer regions in mesh contactor

The mass transfer coefficients for laminar flow in microchannel should be computed to study the absorption rate. Generally, the liquid-side mass transfer coefficients (k_L) are calculated for knowing the absorption rate in the microchannel

because the mass transfer resistance on the liquid side is much higher than gas side and microchannel is applied to reduce mass transfer resistance. So, the liquid-side mass transfer coefficients is obtained to represent the absorption rate in the microchannel.

The average mass transfer coefficients can be used to compute the total gas absorption rate. The average flux ($N_{A,av}$) can be used with some mean concentration difference.

$$N_{A,av} = k_L(C_{i,L} - \bar{C}_L)_M \quad (2.5)$$

The average flux is the different molar flow rate of the component in the liquid per contact area. Then,

$$\frac{Q_L(C_{L,out} - C_{L,in})}{A} = k_L(C_{i,L} - \bar{C}_L)_M \quad (2.6)$$

The logarithmic average of the different at the inlet and outlet of the microchannel is required

$$(C_{i,L} - \bar{C}_L)_M = \Delta C_M = \frac{(C_{i,in} - C_{L,in}) - (C_{i,out} - C_{L,out})}{\ln((C_{i,in} - C_{L,in}) / (C_{i,out} - C_{L,out}))} \quad (2.7)$$

Then, the liquid-side volumetric mass transfer coefficients can be calculated as following equation

$$k_L a = \frac{Q_L(C_{L,out} - C_{L,in})}{V \Delta C_M} \quad (2.8)$$

where a is a specific interfacial area.

2.7 Pressure drop in microchannel

The pressure drop in the microchannel is considered in a rectangular cross-section gas and liquid channel as shown in Figure 2.7 and it can be derived from the Navier – Stokes equation.

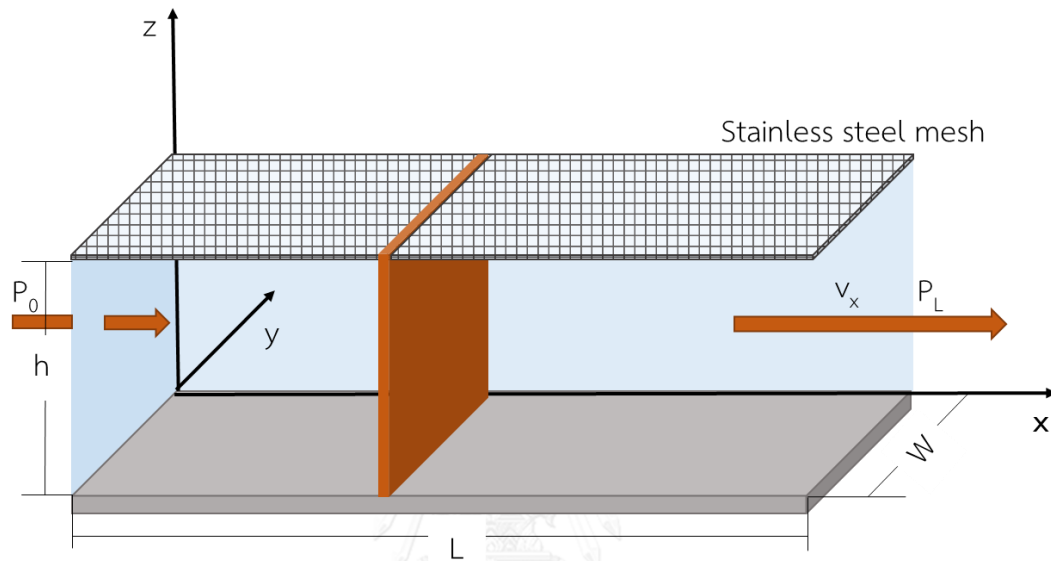


Figure 2.7 Scheme of momentum balance in gas and liquid channel

Assumptions:

1. Steady – state flows in channel.
2. Laminar flow and isothermal.
3. Newtonian fluid
4. No slip condition
5. No convection in y and z direction ($v_y, v_z = 0$)
6. The opening pores of stainless steel mesh were negligible.

So, $v_x = f(y,z)$

x – component:

From Navier – Stokes equation

$$\rho \left(\frac{\partial v_x}{\partial t} + v_x \frac{\partial v_x}{\partial x} + v_y \frac{\partial v_x}{\partial y} + v_z \frac{\partial v_x}{\partial z} \right) = - \frac{\partial P}{\partial x} + \mu \left[\frac{\partial^2 v_x}{\partial x^2} + \frac{\partial^2 v_x}{\partial y^2} + \frac{\partial^2 v_x}{\partial z^2} \right] + \rho g_x \quad (2.9)$$

From the assumptions, we know that

$$\frac{\partial v_x}{\partial t} = 0, v_x \frac{\partial v_x}{\partial x} = 0, v_y \frac{\partial v_x}{\partial y} = 0, v_z \frac{\partial v_x}{\partial z} = 0, \frac{\partial^2 v_x}{\partial x^2} = 0 \text{ and } \rho g_x = 0 \quad (2.10)$$

Then

$$\frac{\partial P}{\partial x} = \mu \left[\frac{\partial^2 v_x}{\partial y^2} + \frac{\partial^2 v_x}{\partial z^2} \right] \quad (2.11)$$

We consider that $\frac{\partial P}{\partial x} = C_0$

The first-order differential equation may be integrated to give

$$P(x) = C_0 x + C_1 \quad (2.12)$$

The first boundary condition is at $x = 0$. It is noted that $P(x) = P_0$ as shown in Figure 2.6

From equation 2.12, we find that

$$P_0 = C_1 \quad (2.13)$$

The first boundary condition is at $x = L$. It is noted that $P(x) = P_L$ as shown in Figure 2.5

From equation 2.12, we find that

$$P_L = C_0L + C_1 \quad (2.14)$$

C_1 in equation 2.13 substitutes in equation 2.14

$$\frac{P_L - P_0}{L} = C_0 \quad (2.15)$$

Finally,

$$-\frac{P_0 - P_L}{\mu L} = \left[\frac{\partial^2 v_x}{\partial y^2} + \frac{\partial^2 v_x}{\partial z^2} \right] \quad (2.16)$$

and

$$v_x = 0 \quad (\text{no slip condition}) \quad (2.17)$$

The Navier – Stokes equation and the boundary conditions for the rectangular cross-section microchannel are shown in Figure 2.8 and following equation.

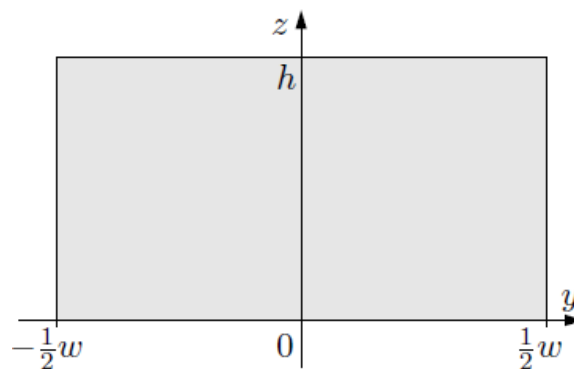


Figure 2.8 Scheme of the boundary conditions of the rectangular cross-section channel [18]

$$-\frac{P_0 - P_L}{\mu L} = \left[\frac{\partial^2 v_x}{\partial y^2} + \frac{\partial^2 v_x}{\partial z^2} \right], \text{ for } -\frac{1}{2}W < y < \frac{1}{2}W, 0 < z < h, \quad (2.18)$$

$$v_x = 0, \text{ for } y = \pm \frac{1}{2}W, z = 0, z = h \quad (2.19)$$

This equation is solved by Bruus, H. [18] and the approximate result of the pressure drop in rectangular cross-section channel is shown in equation 2.20.

$$\Delta P = \frac{12\mu L Q}{h^3 W} \left[\frac{1}{1 - 0.630 \frac{h}{W}} \right] \quad (2.20)$$

where ΔP is a pressure drop in rectangular cross-section channel ($\text{kg/s}^2\text{m}$, Pa), μ is a viscosity of fluid (kg/s.m , Pa.s), L is a length of channel (m), W is a width of channel (m), h is a height (m) and Q is a fluid flow rate (m^3/s).

2.8 Literature reviews

The absorption process between gas and liquid solvent in microchannel have been studied in many researches because it can improve the efficiency. Moreover, microchannel is used in diverse engineering application because improve process control, safety, and reduce the overall size. There have different type of microchannel which are studied for absorption gas by using liquid solvent. Moreover, many parameters are varied to study removal efficiency or mass transfer coefficient in microchannel.

Mass transfer in liquid solvent can be increased by fabricating structure in falling film contactor microchannel. H.monnier et al. (2010) studied an absorption of volatile organic compound in falling liquid film stability microchannel and developed microstructure to protect breaking of liquid film by gas. They found that liquid would

be broken when the liquid flow rate was lower than the minimal liquid flow rate. The liquid was broken by gas causes a dry zone which decreased the interfacial area. For using microstructure, the efficiency was suitable at small liquid flow rates [4].

Dispersed-phase microcontactor is used for absorption process. Ye et al. (2013) studied carbon dioxide absorption by monoethanolamine solutions in T- type rectangular microchannel. In this work, gas and liquid solvent were directly contacted and gas was dispersed into liquid solvent within rectangular microchannel. They found that the removal efficiency of carbon dioxide will yield better if the operating conditions are high temperature, high pressure, high concentration of monoethanolamine solutions. Moreover, the removal efficiency of carbon dioxide in microchannel increase with decreasing aspect ratio because reducing of aspect ratio lead to decreasing of dimension of microchannel which is benefit for mass transfer between gas phase and liquid phase [14].

Mesh contactor is used to investigate absorption between gas and liquid solvent. A. Constantinou et al. (2012) studied carbon dioxide absorption via silicon nitride mesh contactor in microchannel and found that mesh could be used to stabilize gas and liquid interface and keep two phases completely separated. Moreover, the carbon dioxide removal efficiency increased with increasing liquid flow rate and decreasing gas flow rate. The height of liquid channel did not affect carbon dioxide removal efficiency. In addition, the small mesh thickness along with the small pores spaced closely together made the resistance to mass transfer very small [16].

However, the mass transfer coefficient and polarity of mesh were not studied. Simple structure microcannel can increase removal efficiency of carbon dioxide. H. Ganapathy et al. (2014) studied fluid flow and mass transfer characteristics of carbon dioxide absorption in circular cross-sectional minichannel reactor. They found that flow pattern in circular cross-sectional minichannel reactor could be clasified in to five pattern; slug flow, slug-annular flow, annular flow, and churn flow. The slug –annular and churn flow had high specific interfacial area. The absorption efficiency was close to 100% in circular cross-sectional minichannel reactor. Moreover, the mass transfer coefficient was found to be higher when reduce channel length [19].

Microporous in microchannel can generate small bubble which can increase removal efficiency. M. Pan et al. (2015) studied absorption of hydrogen sulfide from a gas mixture in a microporous tube-in-tube microchannel reactor. The microporous tube was allowed gas inlet to flow radially through the micropores into the annular channel which had liquid solvent. They found that the hydrogen sulfide removal efficiency up to 99.85% and the hydrogen sulfide removal efficiency increased with decreasing size of micropore because small micropore formed small gas bubble which led to high interfacial area [20].



CHAPTER III

EXPERIMENTAL

In Chapter 3, it describes apparatuses in this work and experimental procedure of absorption of volatile organic compound in microchannel. This chapter is divided into four main parts including chemicals, microchannel apparatus, experimental setup and procedures, and analytical instrument.

3.1 Chemicals

Toluene which was used as a representative of a volatile organic compound was purchased from Fisher Scientific. Vegetable oil, that was 100% of sunflower oil, was used as a liquid solvent to absorb volatile organic compound. Air zero, purity 99.999%, was used to prepare Toluene/Air mixture. The hydrophobic substance was purchased from Meguiar's.

3.2 Microchannel apparatus

The microchannel in this work consisted of the two Teflon sheets, stainless steel mesh, and two stainless steel plates. It was depicted schematically in Figure 3.1. The stainless steel mesh was in the middle of the microchannel to protect dispersion of gas into the liquid solvent. It was covered by Teflon sheet on top and bottom. The thickness of mesh number 50, 100, 200 and 300 were 0.38, 0.22, 0.12 and 0.08 millimeters, respectively. The thickness of Teflon sheet is 250 μm . The middle of Teflon sheet was cut a hexagonal hole (3 mm length, 1.5 mm width) to be gas and liquid channels. Then, the two stainless steel plates covered a stainless steel mesh and two Teflon sheets and they were clamped tightly with screws. Each stainless steel plate had two holes for inlet and outlet of gas and liquid.

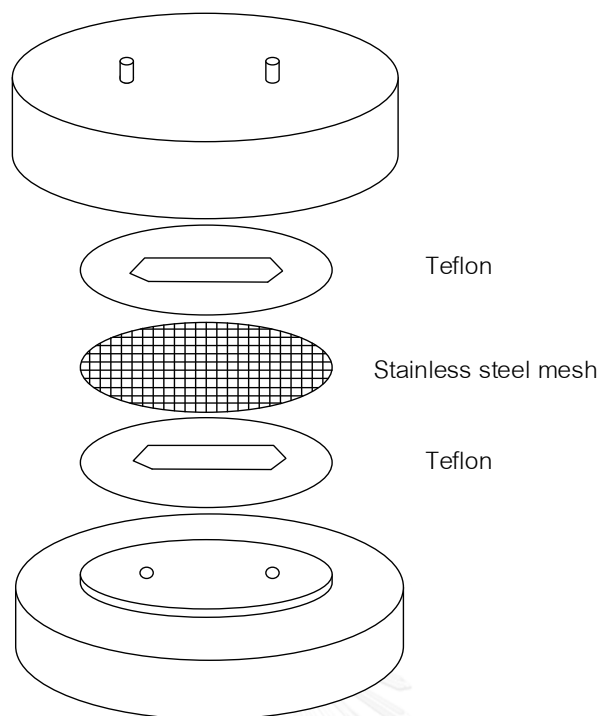


Figure 3.1 Scheme of the microchannel

3.3 Experimental setup and procedures

The experimental setup is shown in Figure 3.2. The purity air (1) was fed into the flask of pure toluene and controlled the gas flow rate by the mass flow controller (2). The toluene gas was generated by bubbling air through the liquid toluene in the flask (3) which was controlled the temperature to keep the constant concentration of toluene gas. The toluene gas from flask was fed into the top of the microchannel (4) while inlet and outlet of liquid solvent, vegetable oil, were closed to check the outlet concentration of toluene gas by Shimadzu 14B gas chromatography. When the outlet concentration of toluene gas is similar to inlet concentration, vegetable oil was pumped into the bottom of the microchannel by a syringe pump (5) to absorb toluene from gas. The outlet gas was collected every 30 minutes for 3 hours.

The flow pattern between gas and liquid solvent can be observed from the outlet of gas and liquid channel to check the separation of gas and the liquid solvent. The flow pattern which gas and liquid solvent are completely separated has

none of bubble gas in the outlet of the liquid channel and none of liquid solvent in the outlet of the gas channel.

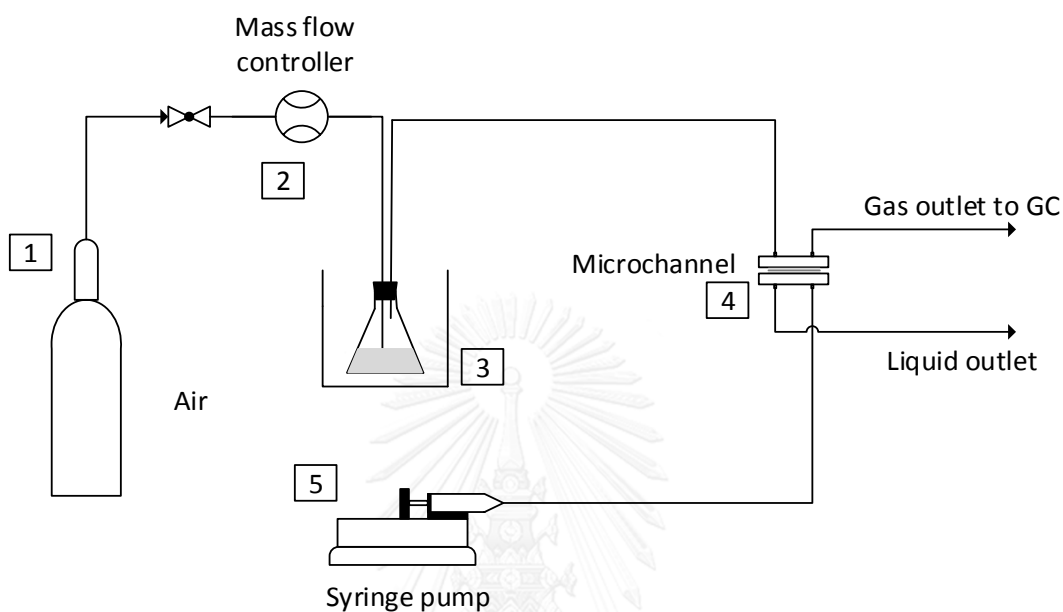


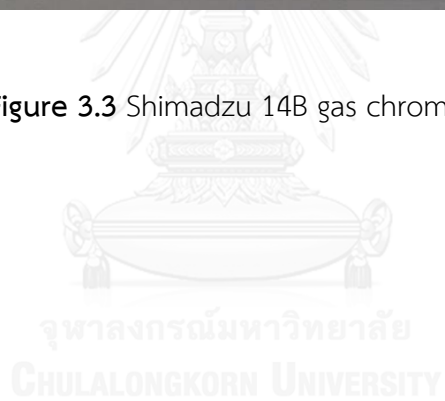
Figure 3.2 Scheme of the experimental setup

3.4 Analytical instrument

The inlet and outlet gas from microchannel were analyzed by using Shimadzu 14B gas chromatograph as shown in Figure 3.3. The gas passed through a polyethylene glycol (PEG-WAX) capillary column and were detected by flame ionization detector (FID) at 250°C. The column initial temperature was 60°C and the final temperature is 90°C with the temperature ramp rate 10°C/min.



Figure 3.3 Shimadzu 14B gas chromatograph



CHAPTER IV

RESULTS AND DISCUSSION

This chapter describes the absorption behavior of VOC gas and liquid solvent in the microchannel by using stainless steel mesh which allows gas and liquid solvent into directly contact with each other without dispersion of one phase into the other. The study of the vapor-liquid equilibrium concentration of toluene and vegetable oil is discussed as Henry's law constant for using vegetable oil as a liquid solvent to absorb VOC. Furthermore, the flow patterns are observed to find the flow pattern regimes which gas and liquid solvent are completely separated. Moreover, the capillary effect in a pore of stainless steel mesh is described the flow pattern regime. Finally, the influence of operating condition parameters on absorption between VOC gas and liquid solvent are studied by using the toluene removal efficiency and the liquid-side volumetric mass transfer coefficient value to describe the absorption behavior.

4.1 Henry's law constant

Henry's law constant of toluene and vegetable oil can be found from equilibrium curve of toluene concentration in gas and vegetable oil as shown in Figure 4.1. It shows the equilibrium concentration of toluene in gas phase and liquid phase at room temperature and atmospheric pressure. In this work, the data of toluene concentration in gas phase in range 0 – 0.0008 mol/l are used to calculate the Henry's law constant because it covers the toluene concentration in this experiment.

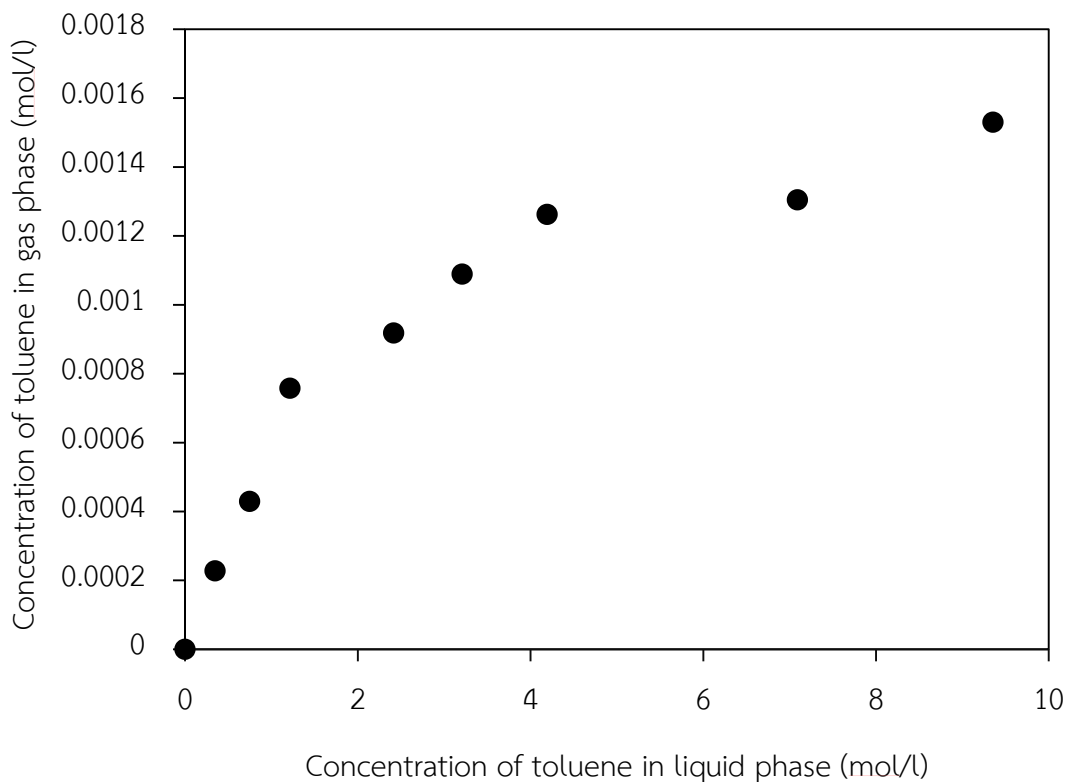


Figure 4.1 Equilibrium curve of toluene concentration in vapor – liquid equilibrium

Henry's law constant from experimental data about concentrations of toluene and vegetable oil in vapor-liquid equilibrium at room temperature and atmospheric are shown in Figure 4.2. It shows the variation of toluene concentration in the gas phase and toluene concentration in vegetable oil in vapor-liquid equilibrium in the range of operation condition. The value of Henry's law constant is determined from the slope of the graph and it is found to be 0.006. Hence, the value of $1/H^*$ is 1667. The liquid with a high value of $1/H^*$ is a proper solvent for the absorption. Vuong et al. reported that oleyl alcohol with the $1/H^*$ value of 1637 is a proper solvent for absorption of VOCs and water with $1/H^*$ value of 4 is not proper for using as a liquid solvent for VOCs. Therefore, vegetable oil is suitable liquid solvent to absorb toluene as it has a high capacity of toluene absorption. This result can be explained by the

structure of vegetable oil which has a long chain of hydrocarbon and high monounsaturated fatty acids content. Moreover, the vegetable oil is a non-polar compound which has a good VOCs absorption capacity. So, vegetable oil is used as a model of the liquid solvent in this work to study the absorption of VOCs in a microchannel with stainless steel mesh.

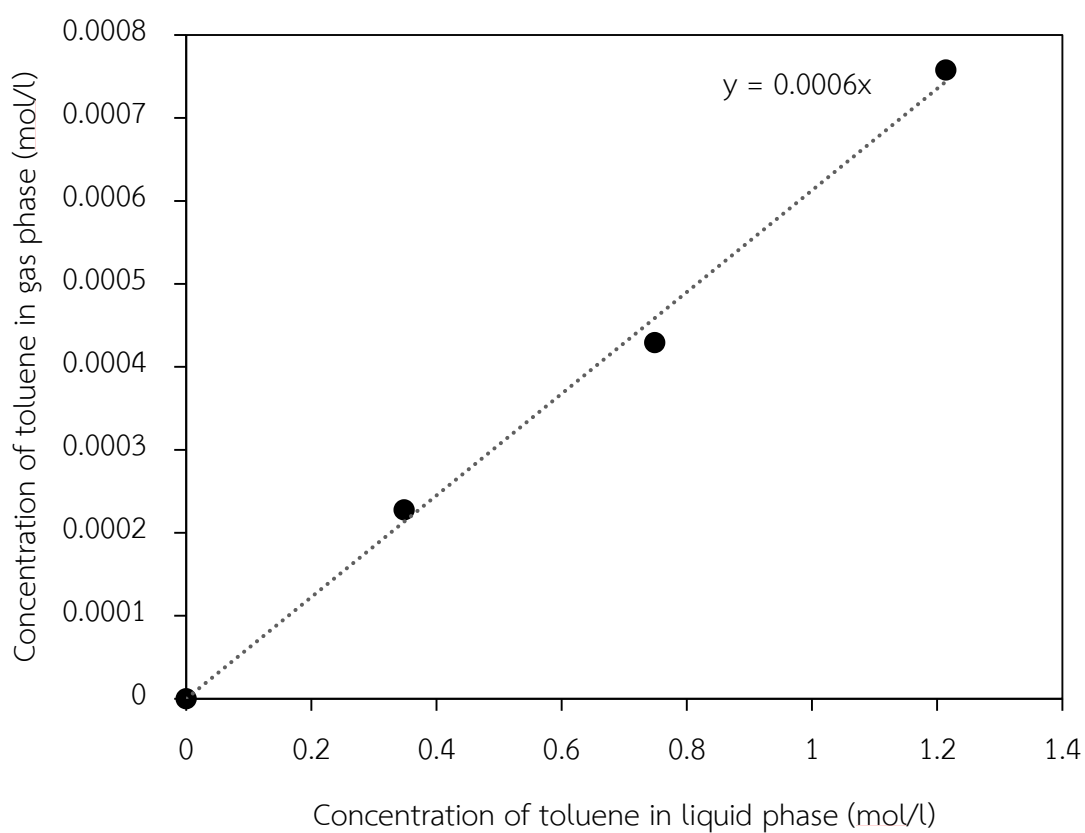


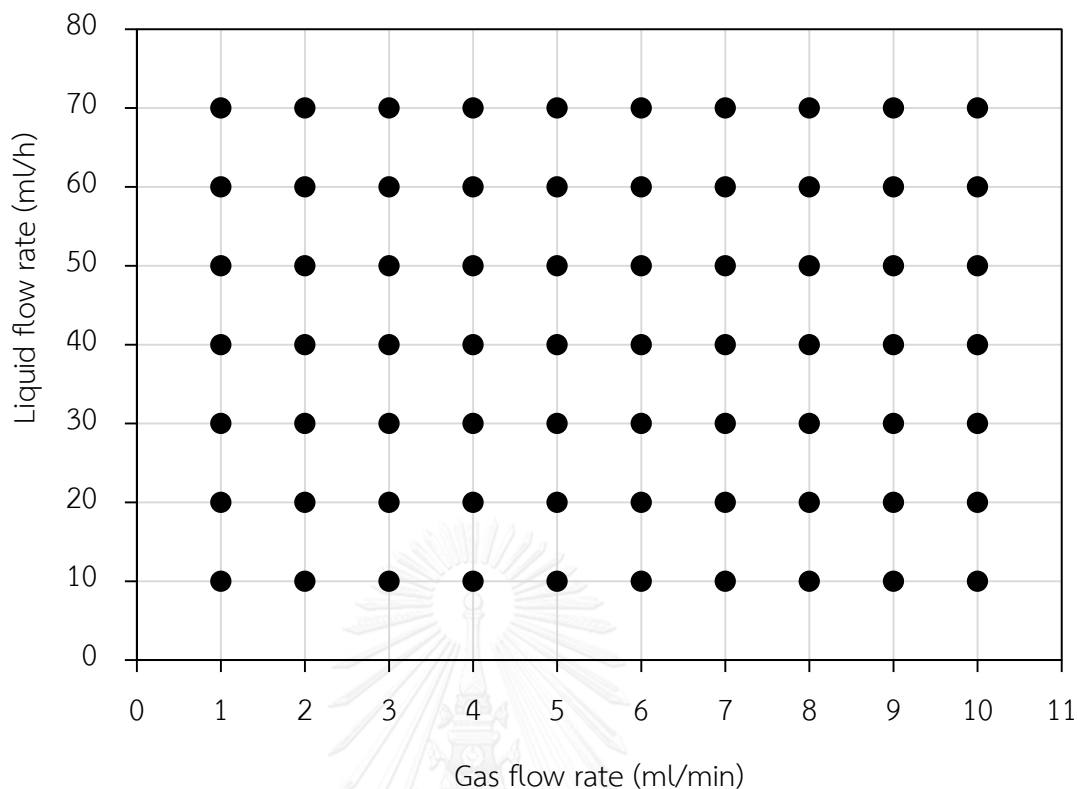
Figure 4.2 Concentrations of toluene and vegetable oil in vapor-liquid equilibrium.

4.2 Flow pattern regime

The flow pattern of gas and liquid phases in a microchannel become different when gas and liquid flow rate are changed. So, the flow pattern regimes are studied for identifying types of flow pattern when the ratios of gas to liquid flow rate are changed. Moreover, the result of flow pattern regimes shows the range of the ratios of gas to the liquid flow rate in each type of flow pattern. In this experiment, the flow pattern regimes between toluene gas and vegetable oil in the microchannel with stainless steel mesh can be classified into three types; (1) gas and liquid solvent are completely separated, (2) gas bubbles are detected in the outlet of liquid solvent, and (3) liquid solvent is detected in the outlet of gas. The flow patterns can be observed from the outlet of gas and liquid channel. If outlet of the liquid channel has gas bubbles in the liquid solvent, it is noted that gas disperses into the liquid solvent. This flow pattern can cause the decreasing of contact area between gas and liquid phase area. The pattern which liquid solvent floods on the mesh can be observed from the gas outlet which is detected liquid solvent in the gas. In this work, it is desired to have on flow pattern which gas and liquid phase are completely separated because it has higher contact area between gas and liquid phase than other patterns.

In this part, stainless steel mesh number 50, 100, 200 and 300 are used to study the flow pattern regimes when pores size of stainless steel mesh are changed because the pores size of stainless steel mesh is relating to the capillary force of vegetable oil within the pores. The pores size of stainless steel mesh number 50 are the largest, 0.356 millimeters, and pores size of stainless steel mesh number 300 are the smallest, 0.044 millimeters.

Figure 4.3 shows flow pattern regime when flow rates of gas and liquid phases are varied, using stainless steel mesh number 50 in the microchannel. According to Figure 4.3, when the mesh number 50 is used, gas disperses into vegetable oil because mesh size is large and the capillary force of vegetable oil within pores of the mesh is small.



- ▲ Gas and liquid solvent are completely separated.
- Gas bubbles are detected in the outlet of liquid solvent.
- Liquid solvent is detected in the outlet of gas.

Figure 4.3 Flow pattern regime between gas and vegetable oil using mesh number 50

When the stainless steel mesh number is increased to 100, gas and vegetable oil are completely separated at a low gas flow rate (see Figure 4.4). Due to small mesh size, the capillary force of vegetable oil within pores of the stainless steel mesh number 100 is higher than the capillary force within stainless steel mesh number 50. At low gas flow rate, gas disperses into vegetable oil at liquid flow rate in range 50 – 70 ml/min because liquid floods on stainless steel mesh at this flow rate and capillary

force of vegetable oil within pores of the mesh does not affect mesh pores. However, when the gas flow rate is 1 - 2 ml/min and the liquid flow rate is 50 – 70 ml/h, gas and vegetable oil are separated because gas cannot penetrate into vegetable oil and blow the vegetable oil out of microchannel at a very low gas flow rate. Moreover, when the gas flow rate is higher than 5 ml/min, vegetable oil is penetrated by gas to form the slug of gas in the liquid channel because high gas flow rate can reduce the capillary force of vegetable oil within pores of stainless steel mesh. From this result, gas disperses into the vegetable oil at gas flow rate 6 – 10 ml/min by using stainless steel mesh number 100 and this lead to decreasing the contact area between the gas and liquid solvent.

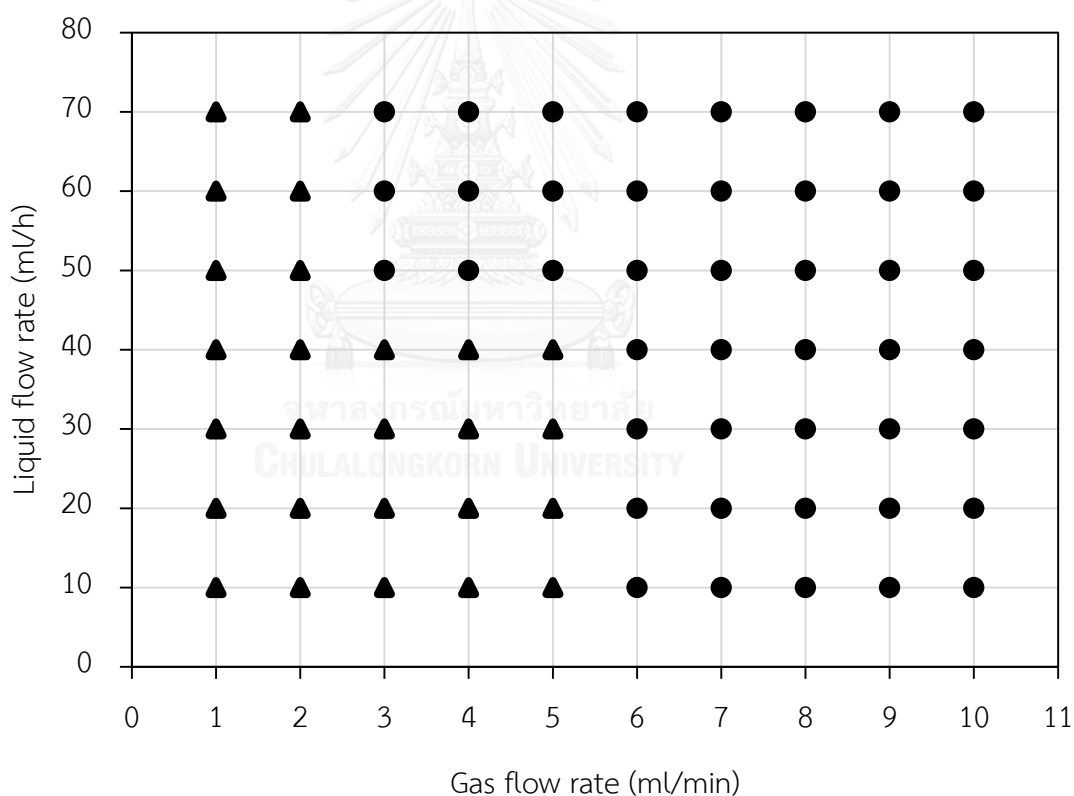


Figure 4.4 Flow pattern regime between gas and vegetable oil using mesh number 100

Gas and liquid solvent can be separated because the pressure of the gas cannot overcome the capillary force within mesh pore. When the gas flow rate is changed to be higher, the pressure of the gas is high. Until the pressure of the gas overcome the capillary force within mesh pore, gas can disperse into the liquid solvent to form a slug of gas.

In this work, the separation of gas and liquid solvent at high gas flow rate is required because high gas flow rate lead to high mass transfer coefficient. And it is supposed that high gas flow rate which has high mass transfer coefficient can reduce volatile organic compounds more than low gas flow rate which has low mass transfer coefficient. So, stainless steel mesh number 200 and 300 are investigated to separate gas and liquid solvent at a higher gas flow rate.

As the stainless steel mesh size is smaller, gas and vegetable oil can be separated at a higher gas flow rate as shown in Figure 4.5. Figure 4.5 shows flow pattern regimes when stainless steel mesh number 200 is used. It shows that stainless steel mesh number 200 can separate gas and vegetable oil at higher gas flow rate when compare with using stainless steel mesh number 100. Due to small pores size, the capillary force of vegetable oil within pores of stainless steel mesh number 200 is higher than stainless steel mesh number 100. Moreover, stainless steel mesh number 200 has another flow pattern which does not appear in stainless steel mesh number 100. It is the flooding of vegetable oil on the stainless steel mesh. This flow pattern occurs when the liquid flow rate is in range 50 – 70 ml/min as same as using stainless steel mesh number 100 which describes above but stainless steel mesh number 200 is different. When vegetable oil floods on stainless steel mesh number 200, gas blows vegetable oil on mesh out of microchannel at high gas flow rate and it can be observed from the outlet of gas which has a bubble of vegetable oil. Because of small pore size and high capillary force, vegetable oil which floods on stainless steel mesh number 200 cannot flow back to liquid channel easily when it is pushed by gas. In addition, when the gas flow rate is higher than 6 ml/min, vegetable oil is penetrated by gas to form the slug of gas in liquid channel. The reason is like using stainless steel mesh number 100 as described before.

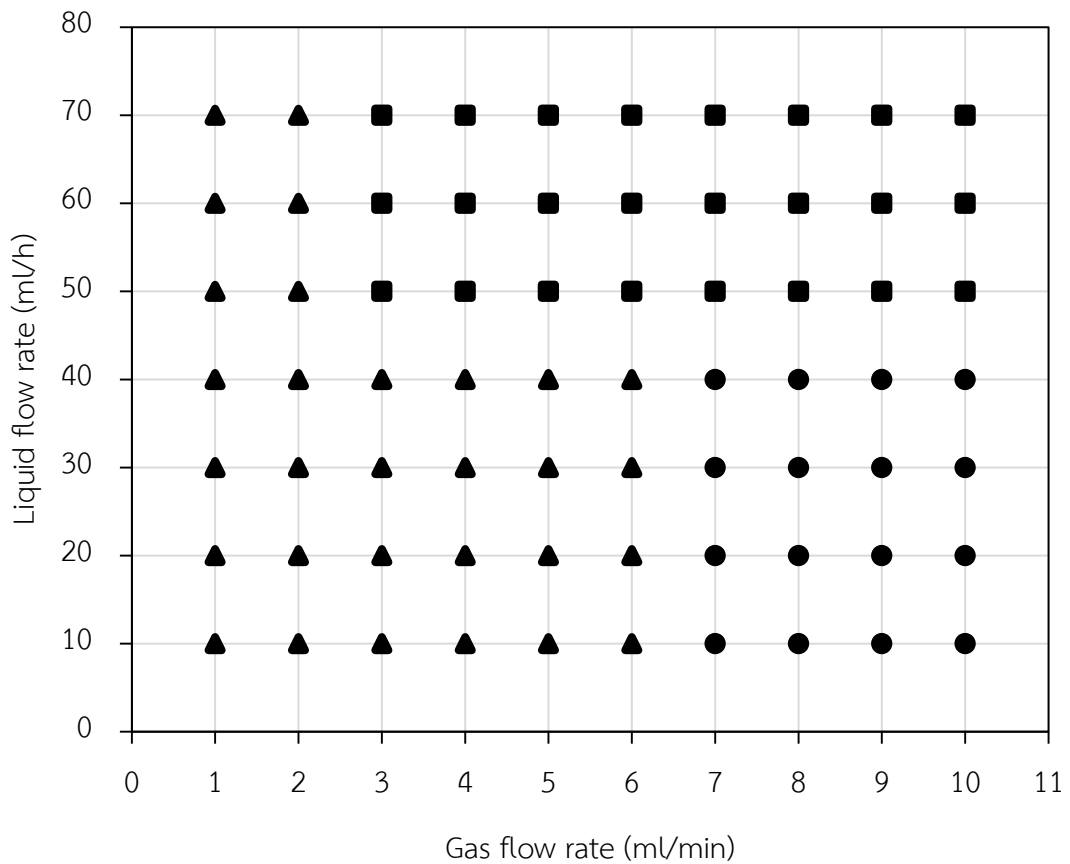


Figure 4.5 Flow pattern regime between gas and vegetable oil using mesh number 200

Figure 4.6 shows flow pattern regimes by using stainless steel mesh number 300. It shows that gas and vegetable oil are completely separated at high gas flow rate because stainless steel mesh number 300 has small pores size and the capillary force of vegetable oil within pores of stainless steel mesh number 300 is high. The flow pattern regime of stainless steel mesh number 300 which gas and vegetable oil are completely separated are wider than stainless steel mesh number 100 because the pores size of stainless steel mesh number 300 are three times smaller than stainless steel mesh number 100. So, the capillary force of vegetable oil within pores of stainless steel mesh is significantly high. In addition, the flow pattern regime which vegetable oil floods on the mesh is narrow when compares with stainless steel mesh number 200. Due to small pore size, vegetable oil is held within pores by capillary force within

pores at a higher liquid flow rate. As you can see from Figure 4.6, gas and vegetable oil are separated at liquid flow rate 50 ml/h which cannot be achieved by using stainless steel mesh number 200.

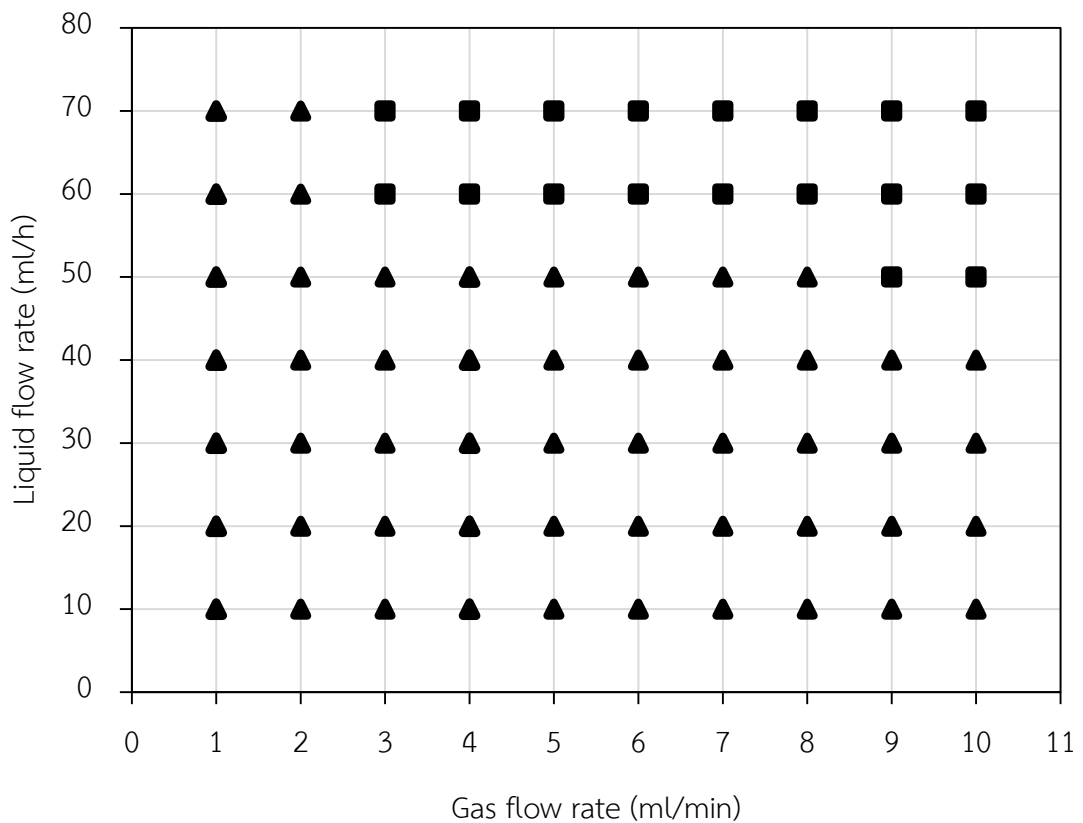


Figure 4.6 Flow pattern regime between gas and vegetable oil using mesh number 300

These results from Figure 4.3 to 4.6 show that mesh size plays a significant role in keeping gas and the liquid solvent separated. The smaller the pores, the higher the capillary force to hold the gas separates from the liquid. Moreover, gas to liquid solvent flow rate ratios are a factor to control separation of gas and the liquid solvent.

4.3 Capillary action

Capillary force of vegetable oil within pores of stainless steel mesh plays a crucial role in keeping gas and vegetable oil separate as described in part 4.2. The capillary force within mesh is the result of cohesion force of liquid molecules and adhesion force of liquid molecules to the solid material to hold a liquid within pores. So, the capillary force within pores of mesh depends on the property of liquid solvent and mesh surface. In this part, the capillary force of vegetable oil within pores of different stainless steel mesh surface is investigated to compare capillary force of vegetable oil within pores of stainless steel mesh and modified stainless steel mesh by coating hydrophobic substance. The property of stainless steel mesh is hydrophilic which has the high capillary force with a polar liquid solvent like water and low capillary force with a non-polar liquid solvent like oil. The hydrophobic stainless steel mesh is used to improve the capillary force of vegetable oil within stainless steel mesh.

The capillary tube is used to study the capillary force of vegetable oil in glass capillary tube which is a representative of hydrophilic material and modified capillary tube which is coated by hydrophobic substance. Moreover, the flow pattern regimes are studied by using hydrophobic stainless steel number 100 and it is compared with unmodified stainless steel number 100 for investigation of the effect of surface stainless steel mesh property on the separation between gas and the liquid solvent.

Figure 4.7 shows the capillary force of water within two different surfaces of glass capillary tube. The glass capillary tube which is coated by hydrophobic substance is on the left and the glass capillary tube which is unmodified capillary tube by hydrophobic substance is on the right. The capillary force of liquid in the capillary tube can be estimated by the surface tension of the liquid and different pressure between two fluids at the interface. Moreover, the comparison of the level of liquid within the capillary tube can indicate which capillary tube has the high capillary force of liquid.

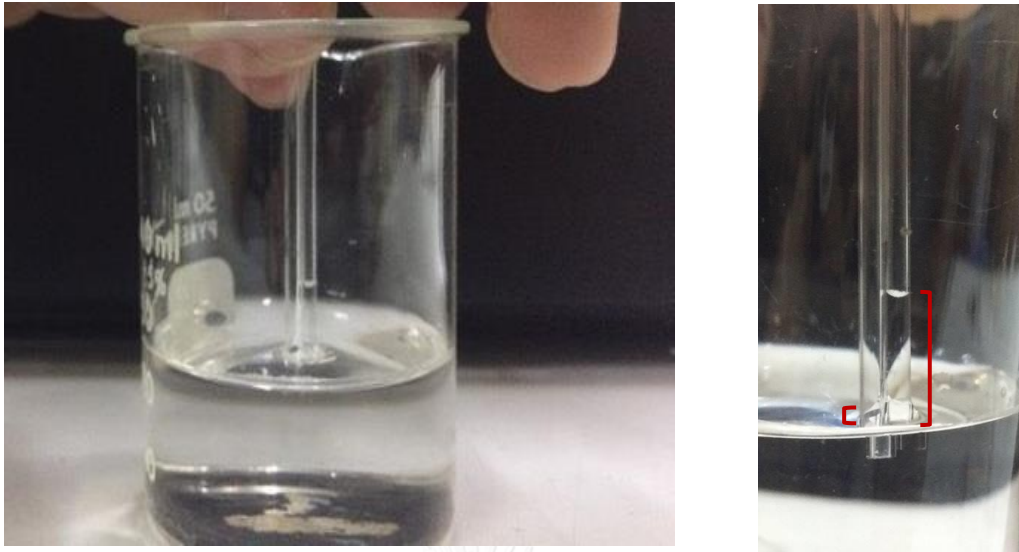


Figure 4.7 Capillary action of water within hydrophobic capillary tube (left) and glass capillary tube (right)

The level of water in Figure 4.7 shows that the capillary force of water within two capillary tubes is significantly different. The capillary force of water within uncoated glass capillary tube is higher than the water within hydrophobic capillary tube because the level of water in glass capillary tube is higher than water in the hydrophobic capillary tube. Moreover, water is a polar liquid which has the high capillary force with a hydrophilic surface like glass. This result can be ensured by the value of surface tension and different pressure of water in the capillary tube.

The surface tension between water and capillary tube surface can be estimated by Young – Laplace equation and the surface tension between water – air and capillary tube surface – air are negligible. The surface tension of water in each capillary tube is shown in Table 4.1. It shows that the value of surface tension between water and glass capillary tube is higher than the hydrophobic capillary tube. It can be ensured that the capillary force within glass capillary is high.

Moreover, the different pressure between water and air within the capillary tube can be calculated by Young – Laplace equation for comparing of the capillary force of water. From table 4.1, it shows that the different pressure between water and air within glass capillary tube is higher than the hydrophobic capillary tube.

Table 4.1 The level, surface tension and different pressure of water within different type of capillary tube.

Type of capillary tube	level of water in capillary tube (m)	Surface tension (N/m)	ΔP (N/m ²)
Glass	0.015	0.070	147
Hydrophobic	0.001	0.0081	9.8

In this work, the vegetable oil is used as a liquid solvent as described in part 4.1. The capillary force of vegetable oil within a different type of mesh is studied by using the capillary tube as shown in Figure 4.8. Figure 4.8 shows the capillary force of vegetable oil within two different surfaces of glass capillary tube. The glass capillary tube which is coated by hydrophobic substance is on the left and the glass capillary tube which is unmodified capillary tube by hydrophobic substance is on the right.

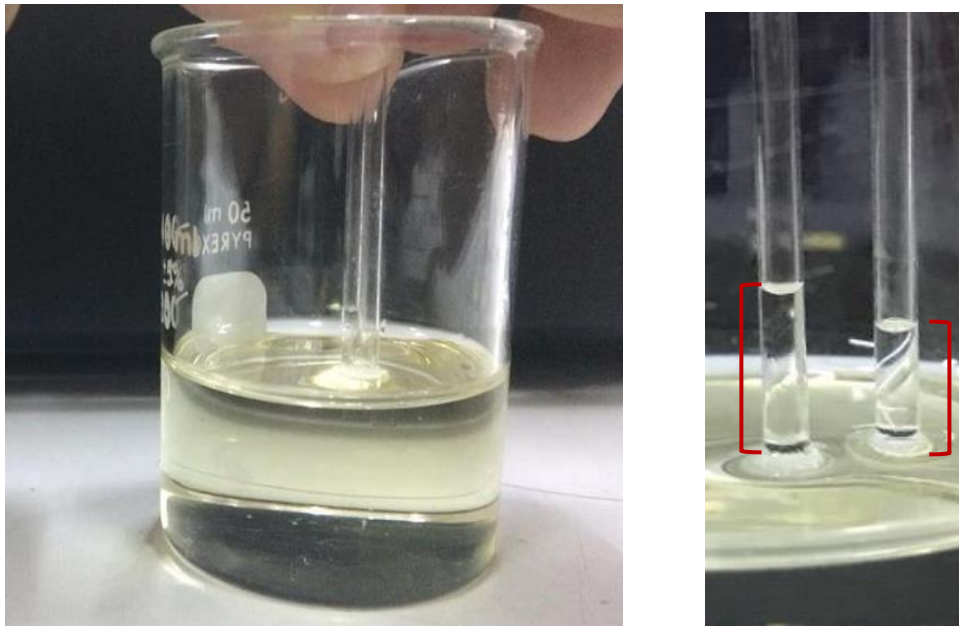


Figure 4.8 Capillary action of vegetable oil within hydrophobic capillary tube (left) and glass capillary tube (right)

The level, surface tension and different pressure of vegetable oil in within two type of capillary tube are shown in Table 4.2. The level of vegetable oil in hydrophobic and glass capillary tube is slightly different because of the properties of the vegetable oil. The surface tension between vegetable oil and the capillary surface is considered and shown that the surface tension of vegetable oil within glass capillary tube is cheap because vegetable oil is a non-polar liquid which has a low capillary force with a hydrophilic surface like glass. Moreover, the surface tension of vegetable oil within hydrophobic capillary tube is higher than glass capillary tube because vegetable oil has the high capillary force with a hydrophobic surface. The capillary force of vegetable oil within two type of capillary tube can be ensured by the different pressure between vegetable oil and air within the capillary tube. It shows that the different pressure between vegetable oil and air within hydrophobic capillary tube is higher than glass

capillary tube. This results can be concluded that the capillary force of vegetable oil within hydrophobic solid channel is high.

Table 4.2 The level, surface tension and different pressure of vegetable oil within different type of capillary tube.

Type of capillary tube	level of vegetable oil in capillary tube (m)	Surface tension (N/m)	ΔP (N/m ²)
Glass	0.006	0.028	54
Hydrophobic	0.008	0.036	72

From the results of the capillary tube, it presents that the capillary force within narrow channel depends on a polarity of the liquid and solid surface. So, the capillary force of liquid solvent within pores of mesh also depends on a polarity of liquid solvent and mesh. Therefore, the flow pattern regimes are changed when a type of liquid solvent and mesh is changed.

The flow pattern regimes of vegetable oil within hydrophobic stainless steel mesh are studied to improve the flow pattern regime which gas and vegetable oil are separated because the capillary force of vegetable oil is high within hydrophobic pores. Figure 4.9 shows stainless steel mesh which is coated with hydrophobic substance is on the left and the hydrophilic stainless steel mesh is on the right. It shows that the hydrophobic stainless steel cannot hold the water within mesh pores because the capillary force of water within hydrophobic solid is low. Unlike stainless steel mesh, it

can hold the water within mesh pores because of hydrophilic property. It is ensured that the stainless steel can be coated by hydrophobic substance.

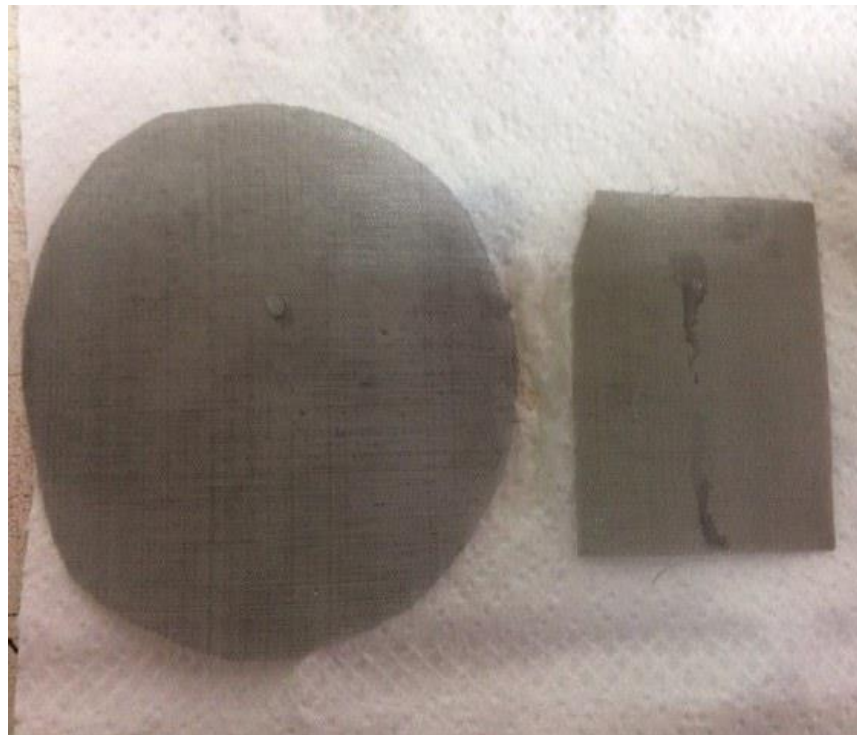


Figure 4.9 Hydrophobic stainless steel mesh (left) and hydrophilic stainless steel mesh (right)

Figure 4.10 shows the flow pattern regimes between gas and vegetable oil using hydrophobic mesh number 100. It shows that the flow pattern regime which gas and vegetable oil are completely separated is wider than using stainless steel mesh number 100 because the capillary force of vegetable oil within hydrophobic pores is increased as described before. The flow pattern regime is gently changed from gas flow rate 5 mL/min to 6 mL/min as shown in Figure 4.4 and 4.10. This changing is not

significant because the capillary force of vegetable oil within hydrophilic and hydrophobic solid pore is slightly different as shown in Table 4.2.

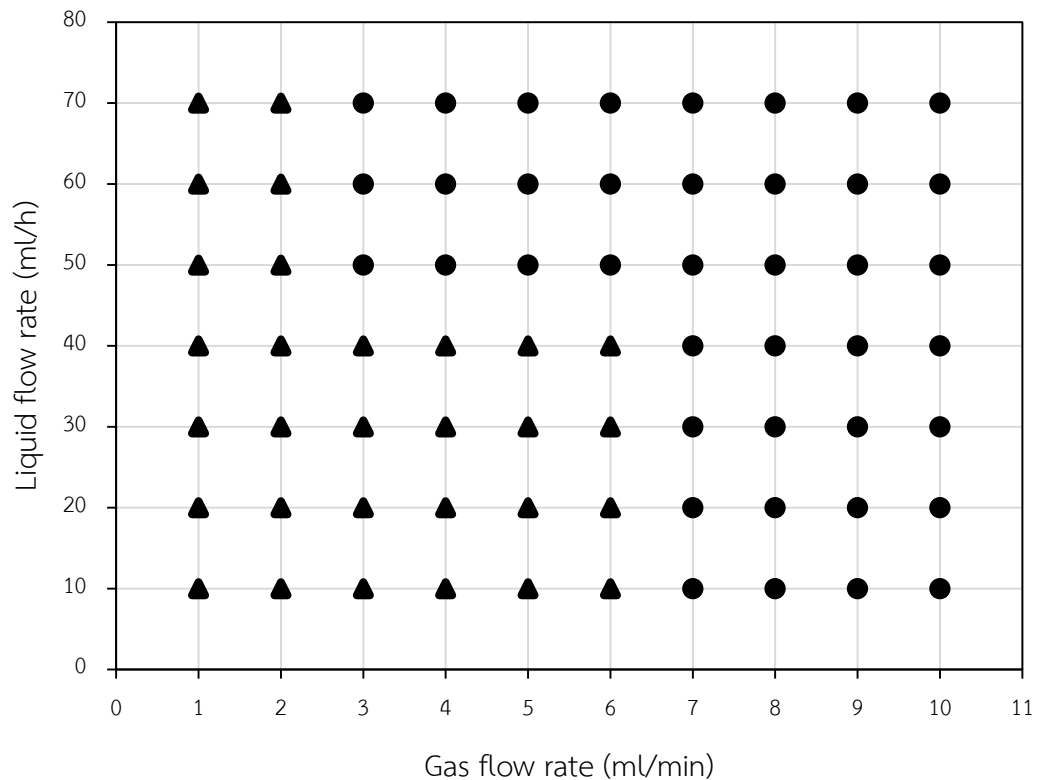


Figure 4.10 Flow pattern regime between gas and vegetable oil using hydrophobic mesh number 100

The results of flow pattern regime show that the improving of flow pattern regime by modifying of stainless steel mesh is worse than using small stainless steel mesh size. It can be described by the different pressure between vegetable oil and air. Table 4.2 shows the comparison of the different pressure between vegetable oil and air within hydrophilic and hydrophobic capillary tube. It shows that the different pressure within hydrophobic capillary tube is slightly higher than the hydrophilic capillary tube. Comparing the different pressure between using modifying of stainless steel mesh and small stainless steel mesh size, it is found that using small stainless

steel mesh size can increase the different pressure dramatically as shown in Figure 4.11. This can be concluded that using small stainless steel mesh is better than modifying of stainless steel mesh for improving the flow pattern regime.

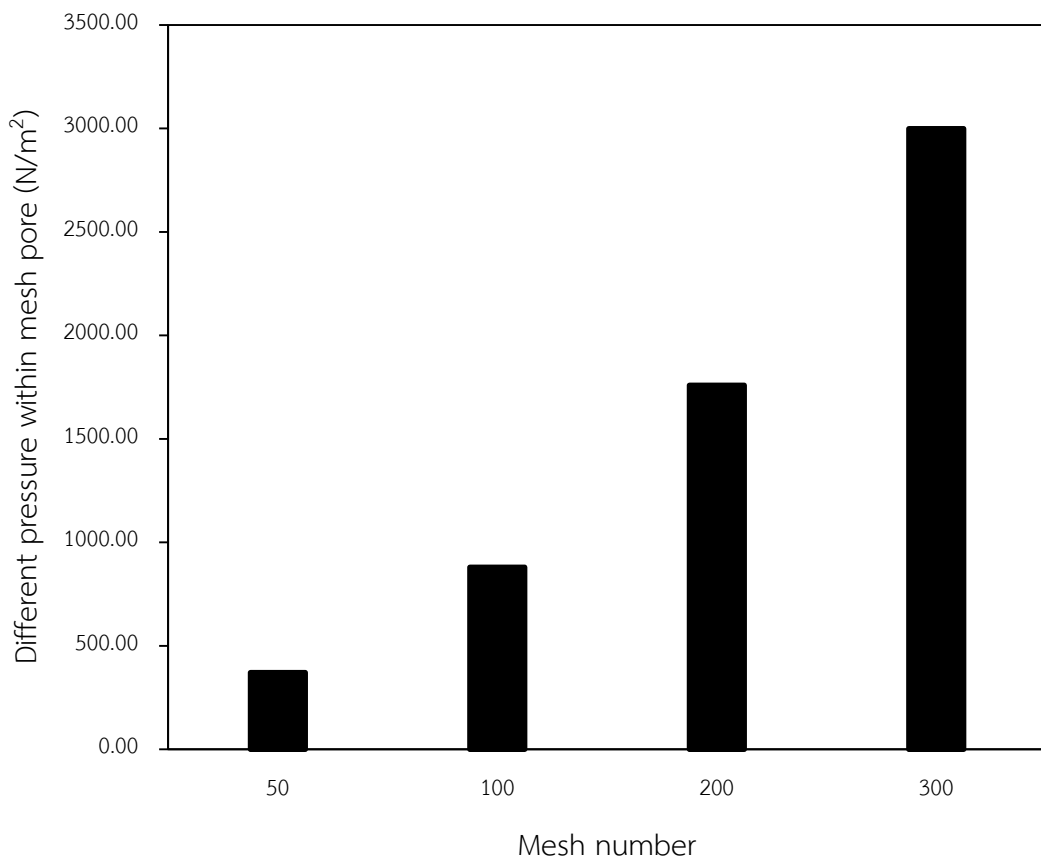


Figure 4.11 Effect of mesh size on the different pressure of vegetable oil

As described above, the capillary force of water within stainless steel mesh is higher than vegetable oil. From this result, gas and water can be completely separated at a high gas flow rate. So, the flow pattern regimes of water are investigated by using stainless steel mesh number 100 to identify the flow pattern regime which gas and water are separated as shown in Figure 4.12. The Figure 4.12 shows that gas and water are separated at high gas flow rate and other flow pattern regime disappears. The result by using stainless steel mesh is similar with using hydrophobic stainless steel

mesh. Moreover, the comparison of flow pattern regime between using vegetable oil and water as a liquid solvent is shown in Figure 4.4 and 4.12. It shows that using of water can handle the separation of gas and liquid solvent at a high gas flow rate.

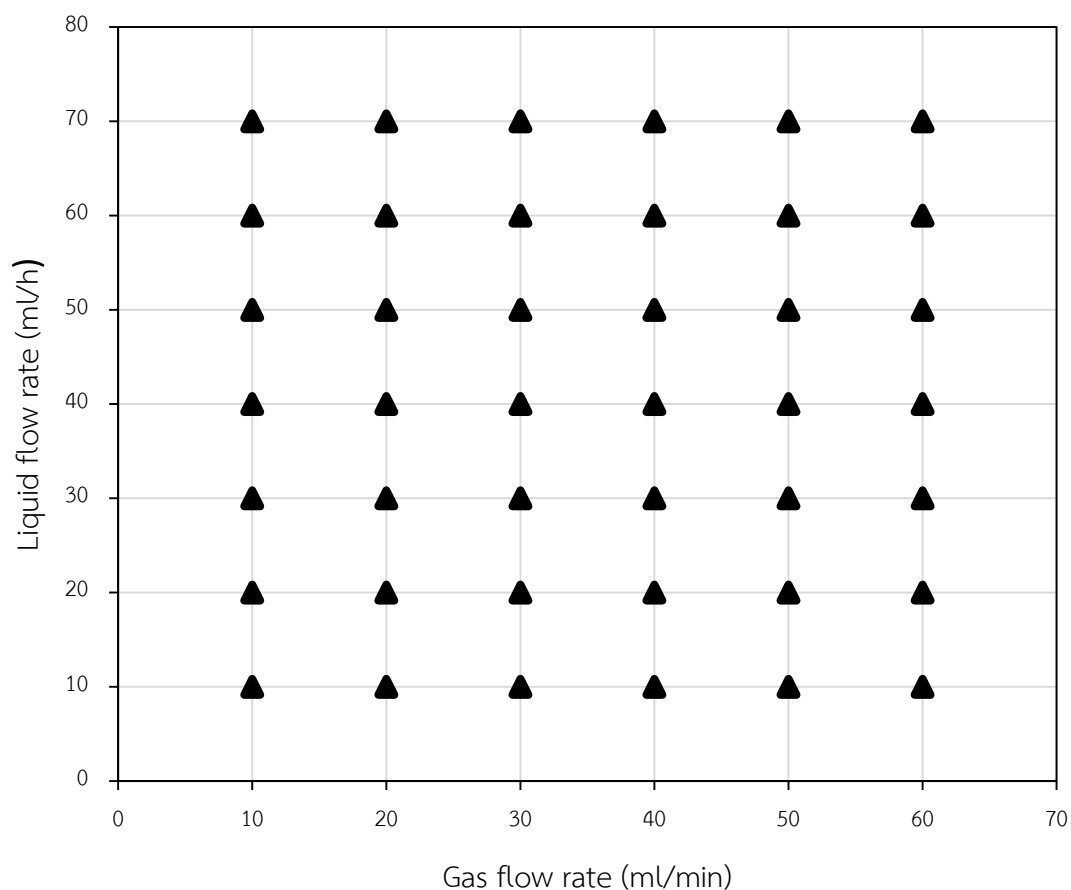


Figure 4.12 Flow pattern regime between gas and water using stainless steel mesh number 100

The result which water can handle the separation of gas and liquid solvent more than vegetable oil at high gas flow rate can be described by the different pressure within mesh pore of vegetable oil and water as shown in Figure 4.13. It shows that the different pressure within mesh pore of water is significantly higher than vegetable oil.

The force between water and glass is higher than using vegetable oil to hold liquid solvent within pores. This ensures that the capillary force of water within stainless steel mesh is higher than vegetable oil. From this reason, water can handle the separation of gas and liquid solvent at a high gas flow rate. However, water is not suitable liquid solvent due to low $1/H^*$ value as described in part 4.1.

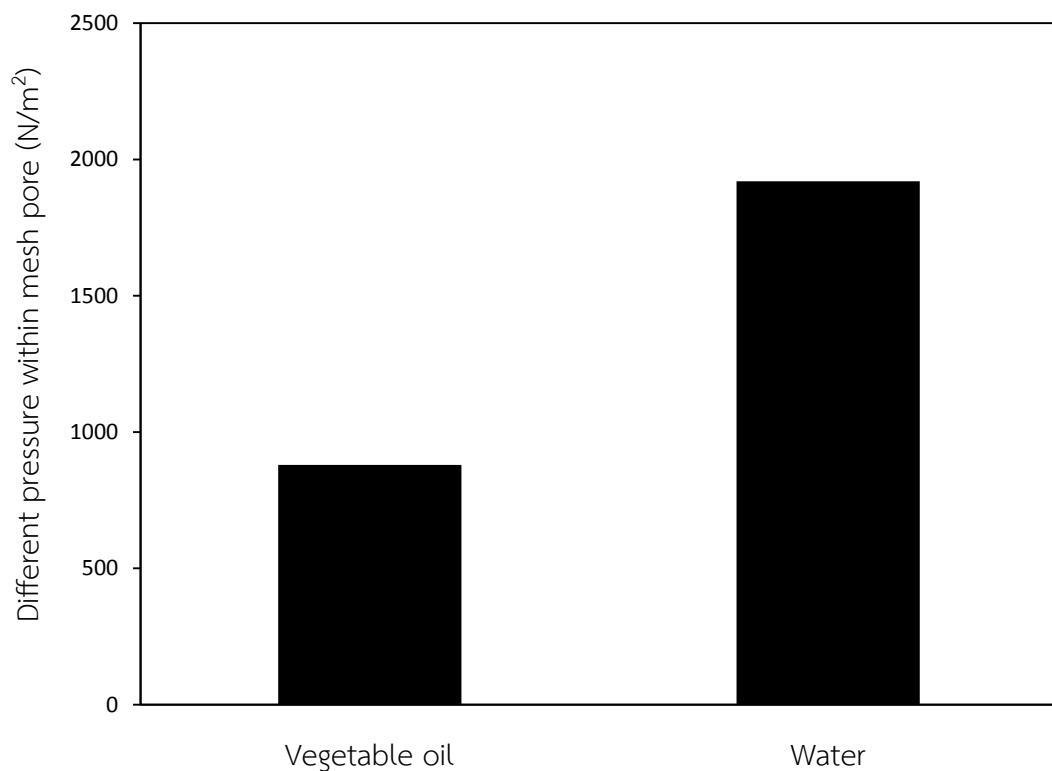


Figure 4.13 Comparison of Different pressure within stainless steel mesh number 100 between vegetable oil and water

4.4 Pressure drop in microchannel

The pressure is a significant role in capillary force of liquid solvent within mesh pores as described in part 4.3. When the pressure is changed, the flow pattern of gas and liquid solvent may be changed. The pressure at inlet and outlet of the microchannel are not equal and it may cause that the flow pattern at each position in the microchannel is not the same. The pressure drop in the microchannel is calculated by H. Bruus equation to find the different pressure between inlet and outlet of the microchannel. Figure 4.14 shows the pressure drop in the gas channel when the gas flow rate is varied from 1 to 10 ml/min. It shows that the pressure drop in microchannel depends on flow rate and it is significantly low when compared with operating pressure which was 101325 Pascal.

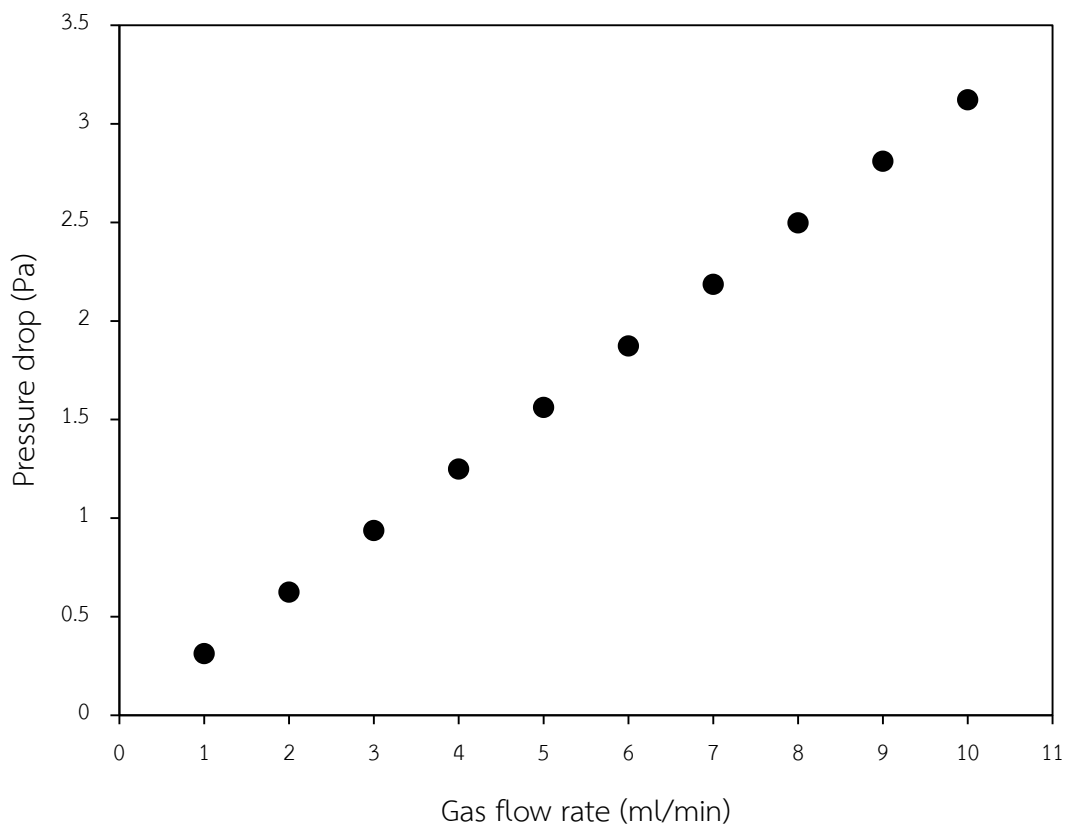


Figure 4.14 Pressure drop in gas channel

This results ensure that the flow pattern at each position in the microchannel is the same because the pressure within microchannel is not very different. Besides, the pressure drop in the liquid channel is calculated and shown in Figure 4.15. From H. Bruus equation, the pressure drop depends on viscosity and flow rate. In this work, vegetable oil is used as a liquid solvent and it has a high viscosity which lead to high the pressure drop in the equipment. Figure 4.15 shows that the pressure drop in the liquid channel by using vegetable oil is low. Even though vegetable oil causes a high-pressure drop in the equipment, the pressure drop in the liquid channel within microchannel is still low. So, the flow pattern in the liquid channel is not changed at each position when the liquid flow rate is unchanged.

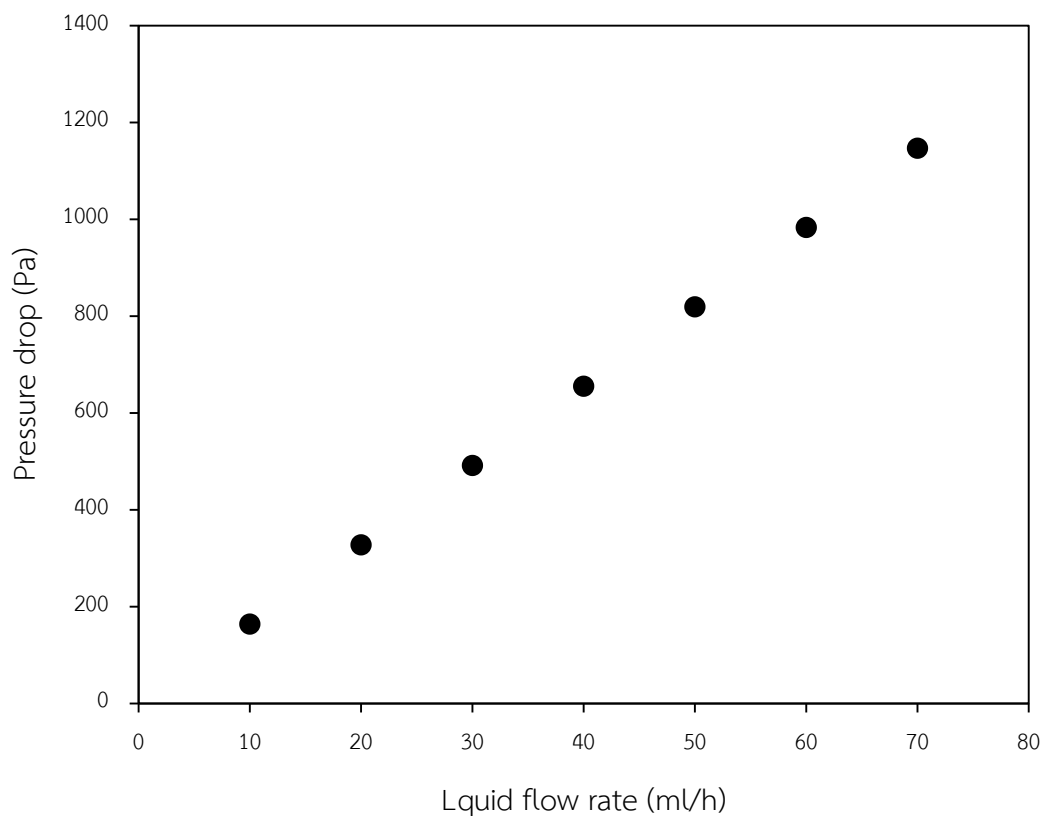


Figure 4.15 Pressure drop in liquid channel

4.5 Absorption

The effect of absorption process behavior of VOCs in the microchannel by using stainless steel mesh is studied to determine the removal efficiency and mass transfer coefficient. In this experiment, toluene is used as representative of VOCs and vegetable oil is used as a liquid solvent. The absorption process is operated in the range which gas and vegetable oil are completely separated. The experimental variables in this part are liquid flow rate, gas flow rate, mesh size, the concentration of gas inlet, channel thickness, channel length and modified stainless steel mesh.

The minimum liquid – gas ratio between toluene and vegetable oil from the experiment is 0.00526 mol vegetable oil/mol dry air. The operating condition which toluene is removed 97 percent in the microchannel is 40 ml/h of liquid flow rate and 5 ml/min of gas flow rate. The liquid – gas ratio in the microchannel is calculated and found that the value of the liquid – gas ratio is 0.98 mol vegetable oil/mol dry air and it is 186 times higher than the minimum liquid – gas ratio. It can be concluded that the liquid – gas ratio in this work must be high for protecting the dispersion of gas and a liquid solvent.

Effect of gas flow rate

The effect of gas flow rate for absorption in the microchannel is studied in 2 centimeters channel length with stainless steel mesh number 100. The liquid flow rate in this experiment is 20 ml/h and the gas flow rate is varied from 3 to 5 ml/min. From the experiment, the system is steady after operating for 90 minutes when the gas flow rate is 5 ml/min and it spends operating time 210 and 240 minutes to access steady system when the gas flow rate is 4 and 3 ml/min. This data shows that the accession of the steady system at high gas flow rate is faster than low gas flow rate. In addition, the effect of gas flow rate on toluene removal efficiency is shown in Figure 4.16. It shows that the toluene removal efficiency at gas flow rate 3 ml/min is higher than gas flow rate 4 and 5 ml/min. The toluene removal efficiency is 93.4, 91.7 and 88.3 when the gas flow rate is 3, 4 and 5 ml/min, respectively. From this results show that low

gas flow rate can reduce VOCs more than high gas flow rate and it is not as expected. From part 4.1, it is expected that high gas flow rate can absorb VOC better than low gas flow rate due to high mass transfer coefficient.

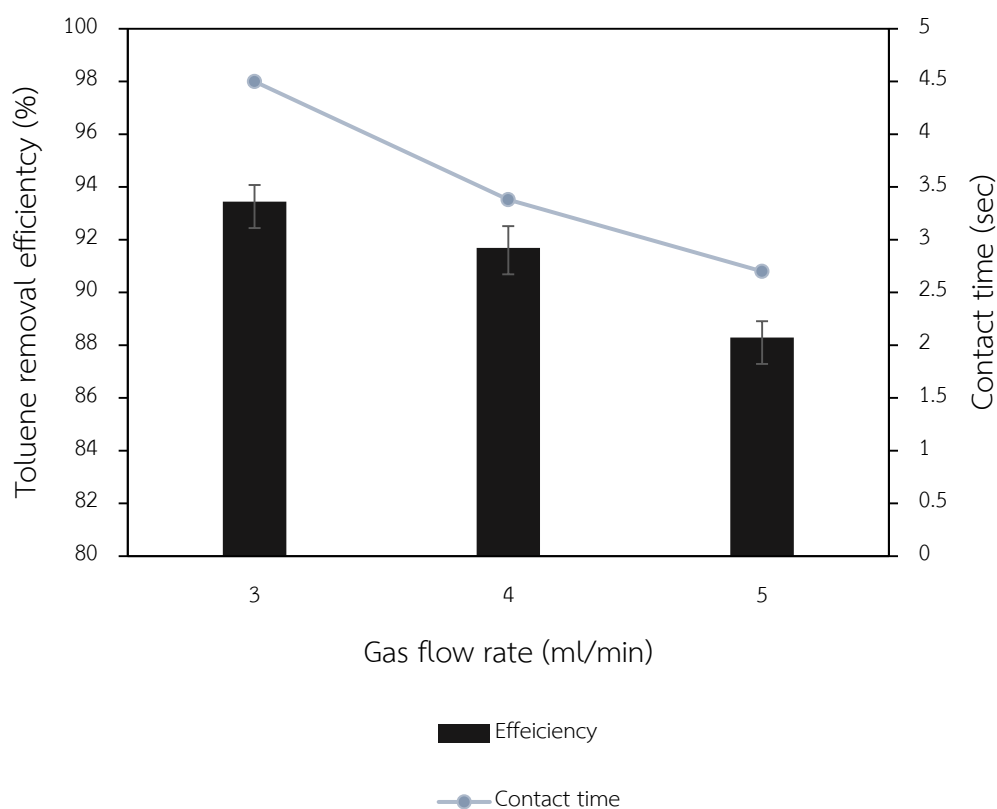


Figure 4.16 Effect of gas flow rate on toluene removal efficiency

The liquid-side volumetric mass transfer coefficients, $k_L a$, from experiments in the microchannel are calculated by equation (2.8) and presented in Figure 4.17. Normally, the gas-side volumetric mass transfer coefficient ($k_G a$) is studied in a conventional absorber because large absorber has a high volume of gas. The high volume of gas prepares the bulk of gas which leads to high mass transfer resistance in the gas phase. So, the limiting mass transfer in a conventional absorber occurs in the gas phase. In this work, the microchannel is applied to reduce the bulk of gas and liquid phase. The limiting mass transfer in the microchannel occurs in liquid phase because the diffusivity of volatile organic compound in the liquid phase is lower than

the diffusivity in the gas phase. So, the liquid-side volumetric mass transfer coefficient is determined in the microchannel. It shows that the liquid-side volumetric mass transfer coefficient increases when the gas flow rate is increased. This results are explained by equation (2.8) which shows that the liquid-side volumetric mass transfer coefficient depends on two terms, the gas flow rate and the different of gas concentration. Even though the low gas flow rate can absorb toluene more than high gas flow rate, the liquid-side volumetric mass transfer coefficient at low gas flow rate is lower than high gas flow rate. So, it is figured out that the gas flow rate plays a crucial role in the liquid-side volumetric mass transfer coefficient.

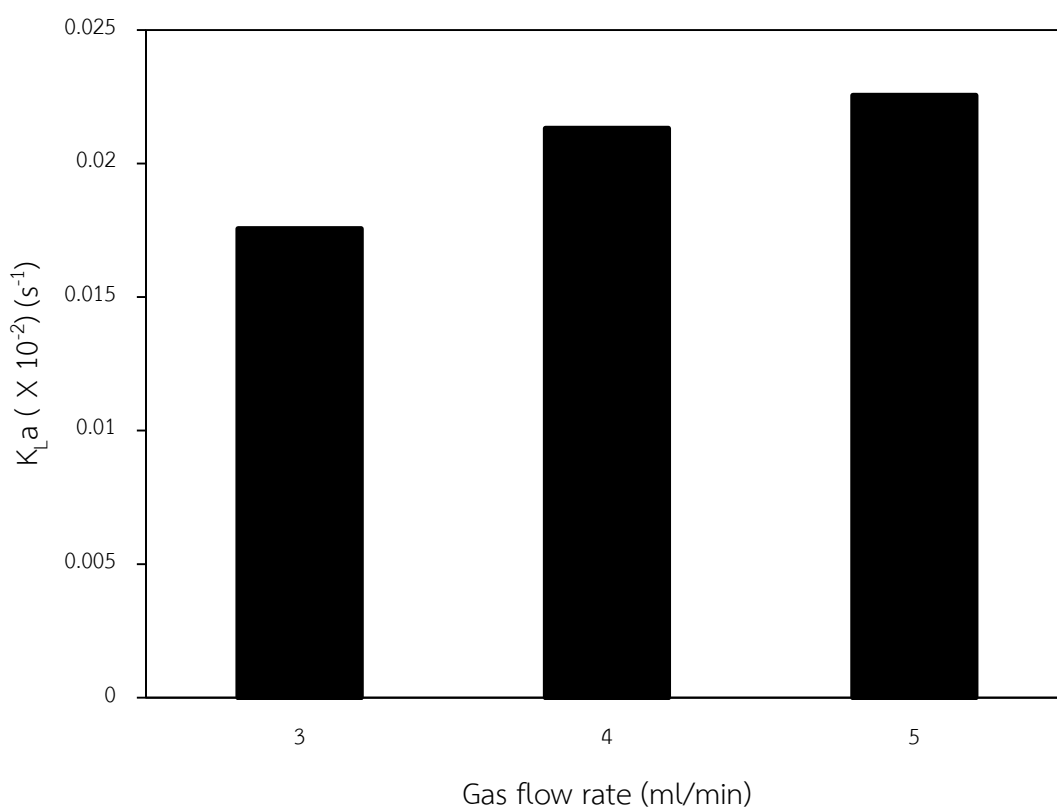


Figure 4.17 Effect of gas flow rate on the liquid-side volumetric mass transfer coefficients

As described above, when the gas flow rate is increased, the liquid-side volumetric mass transfer coefficient increases while the absorption of VOC decreases.

It is realized that the absorption efficiency of VOC in the microchannel is not only up to the liquid-side volumetric mass transfer coefficient but it also depends on the contact time between gas and the liquid solvent. Because of the different of contact time, the toluene removal efficiency is different as you can see in Figure 4.16. In this work, the contact time is a definition of the length of time which gas contacts the liquid solvent in the microchannel. It is calculated from gas flow rate and volume of channel. When the gas flow rate is 3, 4 and 5 ml/min, the contact time between gas and the liquid solvent is 4.5, 3.4 and 2.7 seconds, respectively.

Therefore, the low gas flow rate which has more contact time between gas and liquid solvent lead to the high absorption of VOC in the microchannel.

Effect of liquid flow rate

The effect of liquid flow rate for absorption in the microchannel is studied in channel length 2 centimeters with stainless steel mesh number 100. The gas flow rate in this experiment is 5 ml/min and the liquid flow rate is varied from 20 to 60 ml/min. The effect of liquid flow rate on toluene removal efficiency is shown in Figure 4.18. It shows that the toluene removal efficiency increases when the operating time is less than 90 minutes and after that, it reaches closely to the constant value because the system is steady after operating system more than 90 minutes when the gas flow rate is 5 ml/min. From the graph, the toluene is removed by about 95% at the liquid flow rate of 20 and 40 ml/h. The removal of toluene at the liquid flow rate of 20 ml/h is only slightly higher than that at the liquid flow rate of 40 ml/h regardless of the fact that the contact time between gas and liquid is doubled. This is the result of low mass transfer resistance in the microchannel. As the liquid flow rate is increased to 60 ml/h, the toluene removal efficiency drops significantly. This is due to the incomplete separation between gas and liquid solvent (as shown in Figure 4.4), which reduces the interfacial area.

The liquid-side volumetric mass transfer coefficients from experiments in the microchannel are calculated when the system is steady after 90 minutes and the results are presented in Figure 4.19. It shows that the mass transfer coefficient in liquid

depends on liquid flow rate. The liquid-side volumetric mass transfer coefficient in this work is up to 0.00165 s^{-1} and it is higher than conventional absorbers which have the volumetric mass transfer coefficient in the range of $0.0004\text{--}0.00102 \text{ s}^{-1}$. So, the enhancement of the mass transfer coefficient can be achieved by using microchannel.

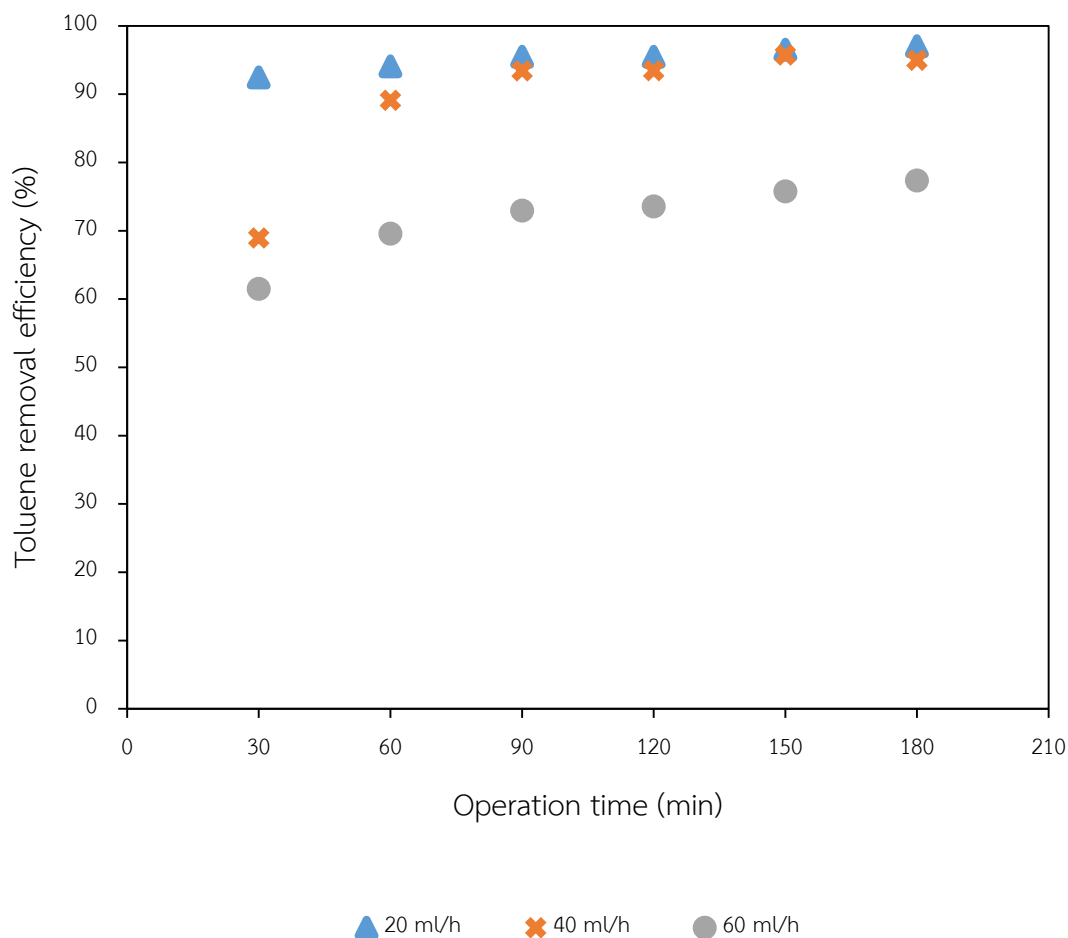


Figure 4.18 Effect of liquid flow rate on toluene removal efficiency

From the results, it is realized that increasing of liquid flow rate does not affect the VOC removal efficiency when gas and liquid solvent are completely separated. Even though increasing of liquid solvent leads to high liquid-side volumetric mass transfer coefficient, the VOC removal efficiency is not different. Due to short contact time in 2 centimeters microchannel, the VOC removal at the liquid flow rate of 20 and

40 ml/h are quite the same value. Moreover, the dispersion of gas into the liquid solvent leads to low liquid-side volumetric mass transfer coefficient and the absorption of VOC is terrible when gas disperses into the liquid solvent as supposed in part 4.1.

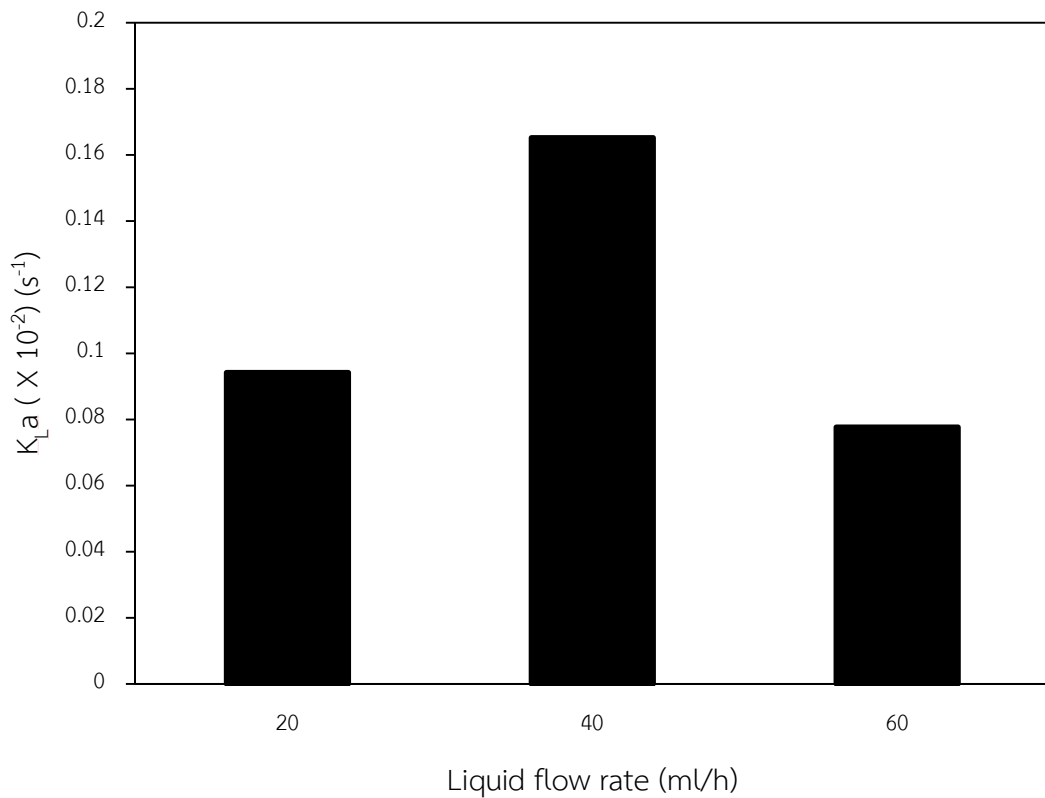


Figure 4.19 Effect of liquid flow rate on the liquid-side volumetric mass transfer coefficients

Effect of channel length

The results of the effect of liquid flow rate by using the 2 centimeters microchannel show the unclear results. So, the channel length is increased to be 6 centimeters to investigate the VOC removal obviously. The effect of channel length for absorption in the microchannel is studied in channel length 6 centimeters with stainless steel mesh number 100. The gas flow rate in this experiment is 5 ml/min and the liquid flow rate is varied from 10 to 40 ml/min which gas and vegetable oil are separated. The pressure drop in 6 centimeters microchannel is calculated and it is

found that the pressure drop in 6 centimeters microchannel is three times higher than 2 centimeters microchannel. However, the pressure drop in 6 centimeters microchannel is still low and the gas and vegetable oil in each position in the microchannel are completely separated. The toluene removal efficiency in 6 centimeters microchannel is shown in Figure 4.20 and it is obviously found that the increasing of liquid flow rate leads to increasing of toluene removal efficiency. As the liquid flow rate increases, the concentration of vegetable oil is kept higher since more fresh vegetable oil is replaced to absorb toluene in the gas phase and it increases the driving force for toluene removal. So, the toluene at high liquid flow rate is absorbed more than low liquid flow rate.

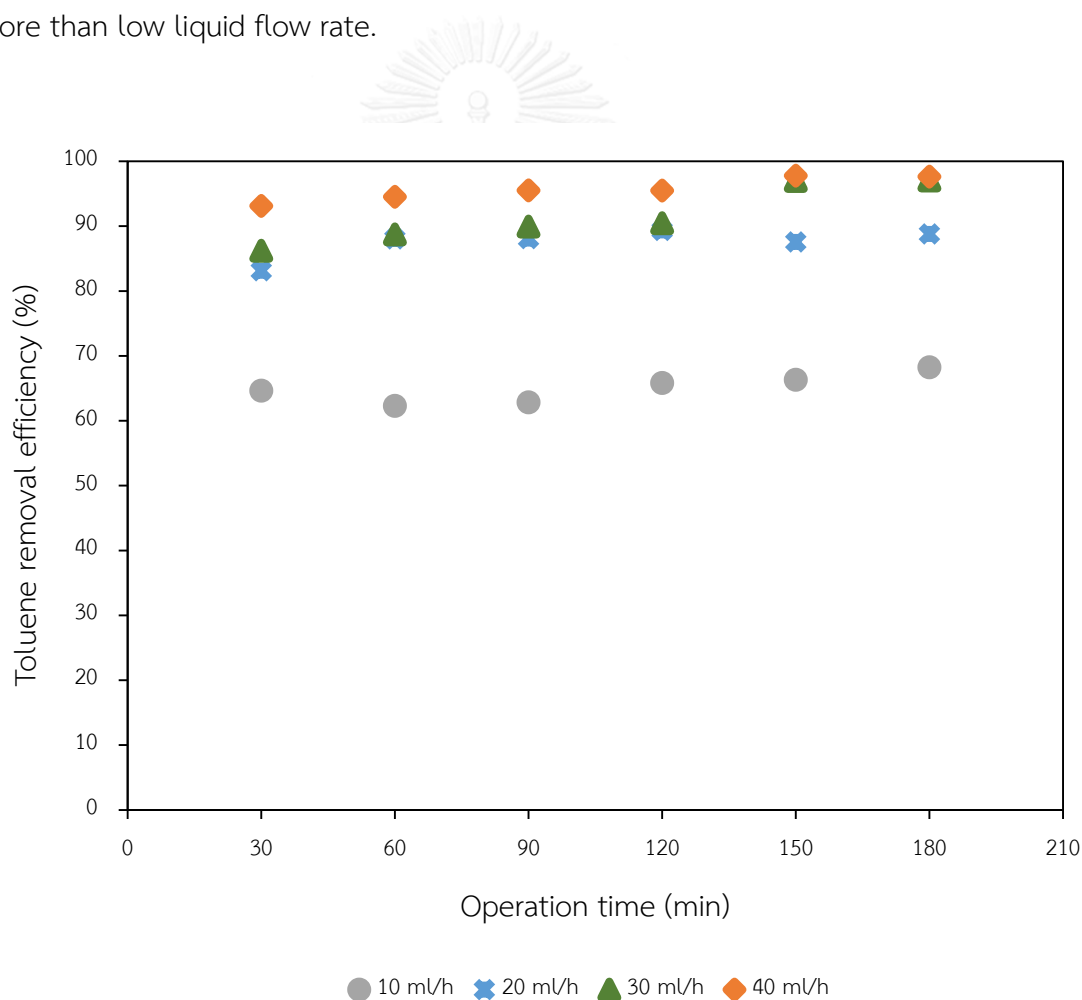


Figure 4.20 Effect of liquid flow rate on toluene removal efficiency by using 6 centimeters microchannel

In addition, the toluene removal efficiency of two size microchannel is compared and it is found that the toluene removal efficiency in 2 centimeters and 6 centimeters microchannel are 95.7 and 97.7 percent when the liquid flow rate is 40 ml/min. Because the increasing of channel length leads to increasing of contact time between gas and the liquid solvent. So, the toluene in the gas phase is absorbed longer when the channel is increased. However, when the liquid flow rate is 20 ml/min, the toluene removal efficiency drops from 96.1 to 88.4 percent when the microchannel is changed from 2 centimeters to 6 centimeter microchannel. This is considered that toluene may be stripped from vegetable oil and the toluene removal efficiency significantly drops. It occurs in the long channel length and low liquid flow rate. The toluene is absorbed into vegetable oil at first and then it is stripped by gas from vegetable oil. Because of the low flow rate of vegetable oil, the vegetable oil flows in the microchannel for a long time until gas stripped the toluene from vegetable oil. Therefore, the toluene removal efficiency in the long microchannel is higher than using short microchannel at high liquid flow rate but it is different when the liquid flow rate is low.

The liquid-side volumetric mass transfer coefficients are calculated and presented in Figure 4.21. It shows that the liquid-side volumetric mass transfer coefficient increases when the liquid flow rate is increased because increasing of liquid flow rate leads to increasing of driving force which toluene is absorbed faster as described above. Although the toluene removal efficiency in 6 centimeter microchannel is higher than using 2 centimeter microchannel, the liquid-side volumetric mass transfer coefficient in 6 centimeter microchannel is low. This can be explained by equation (2.) and it shows that the liquid-side volumetric mass transfer coefficient is a variable inversion with the volume of equipment. So, increasing of channel length leads to increasing volume of the microchannel and decreasing of liquid-side volumetric mass transfer coefficient.

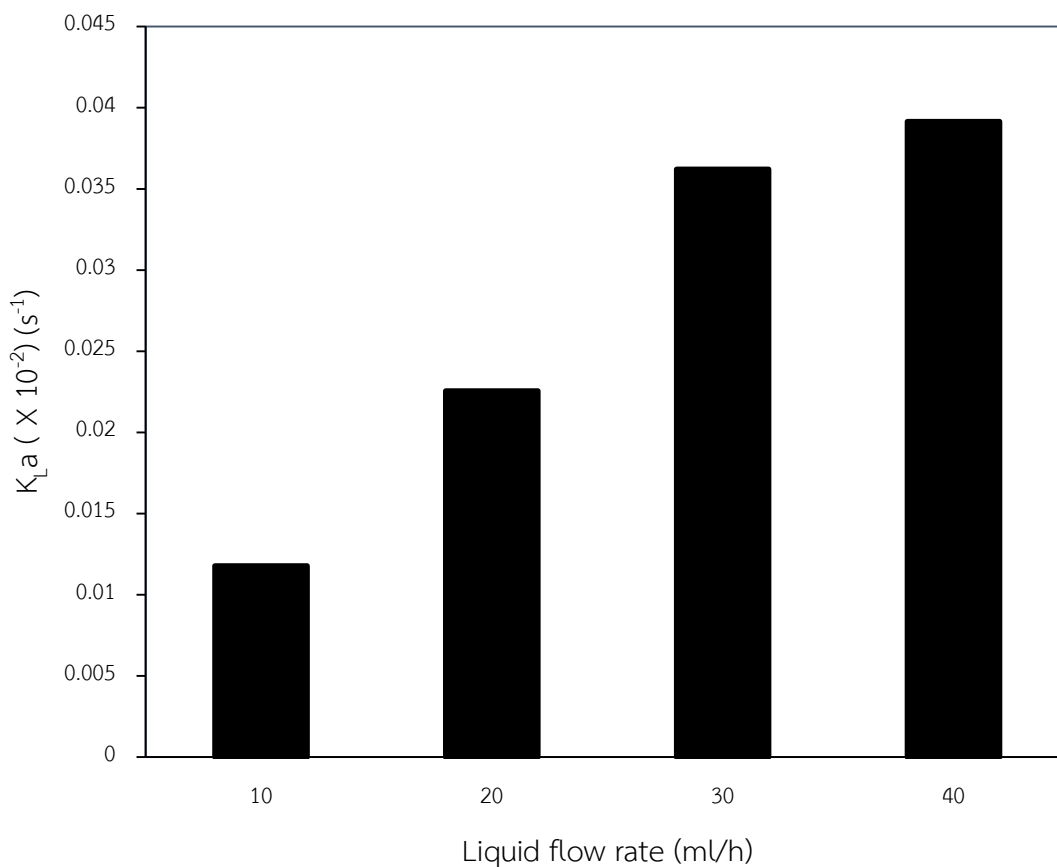


Figure 4.21 Effect of liquid flow rate on the liquid-side volumetric mass transfer coefficients by using 6 centimeters microchannel

Effect of mesh size

The effect of different mesh size is reported in Figure 4.22 and it shows that toluene removal efficiency increases by increasing mesh size or decreasing mesh number. In this experiment, the gas flow rate is 5 ml/min and the liquid flow rate is 20 ml/min. From Figure 4.22, the toluene removal efficiency is 96.1, 69.3 and 62.6 when stainless steel mesh number is 100, 200 and 300, respectively. The operation using mesh number 100 results in higher toluene absorption than when the mesh number is either 200 or 300 because of the reduction in the opening area of the mesh, i.e., mesh number 100 has 35.6 percent opening while mesh number 200 and 300 has 35.0

percent opening and 26.5 percent opening, respectively. Nevertheless, it should be noted that gas and liquid are well separated in these experiments. It is realized that the large mesh size can absorb the VOC more than small mesh size although it cannot handle the separation of gas and liquid solvent at the high gas flow rate.

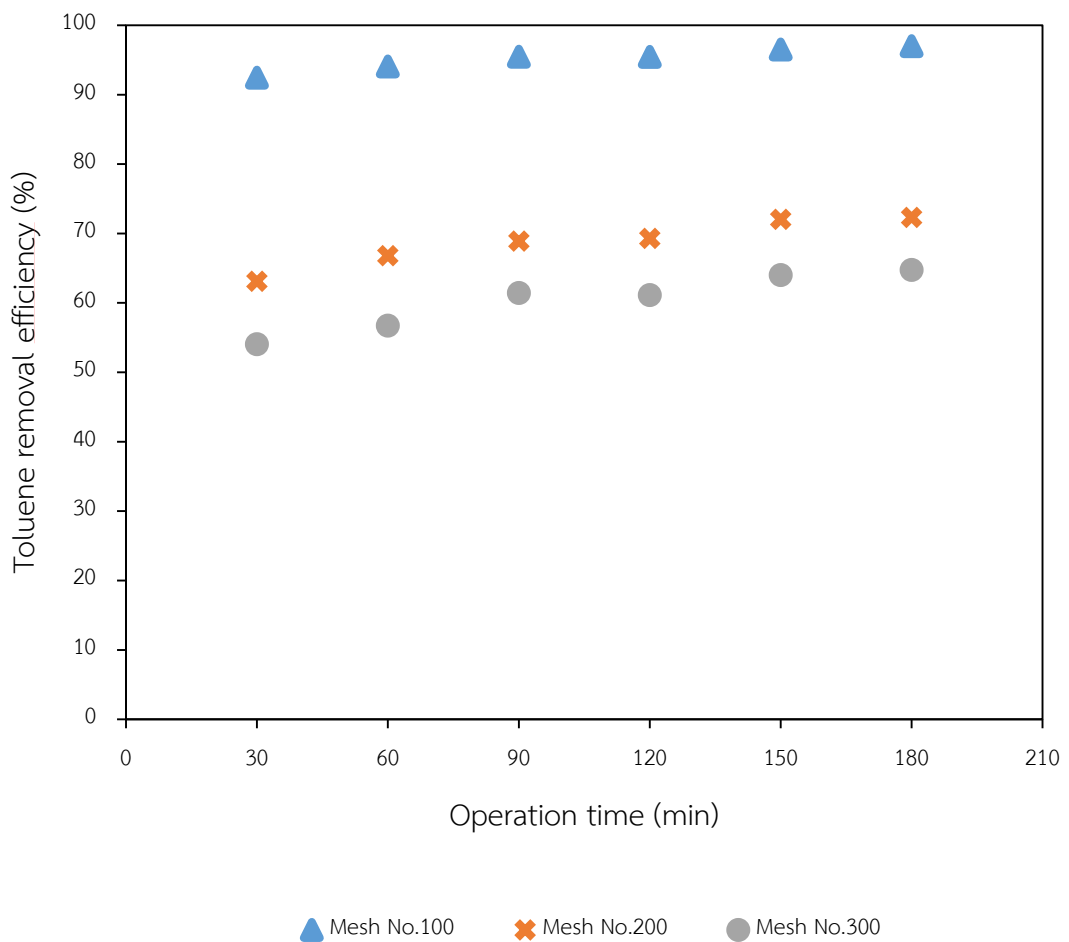


Figure 4.22 Effect of mesh size on toluene removal efficiency

The liquid-side volumetric mass transfer coefficients are calculated and shown in Figure 4.23. It shows that the liquid-side volumetric mass transfer coefficient is high when the large mesh size is used because the flow rate of gas and vegetable oil are

fixed and the liquid-side volumetric mass transfer coefficient only depends on the different of liquid concentration term which is high by using large mesh size.

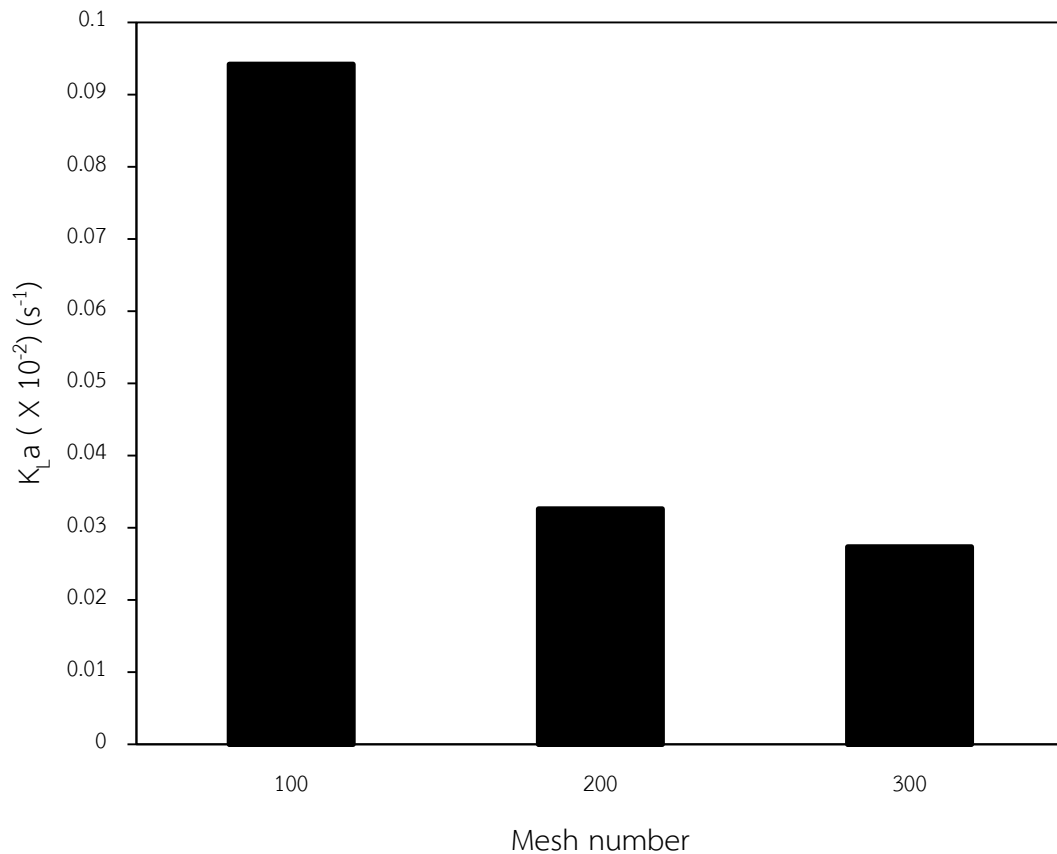


Figure 4.23 Effect of mesh size the liquid-side volumetric mass transfer coefficients

Effect of channel thickness

The different channel thickness of gas and liquid channel are studied for the absorption of VOC. In this work, the channel thickness of gas and liquid are 250, 500 and 750 microns. The channel thickness have to less than 1000 microns because it is in the range of microchannel. The gas flow rate in this experiment is 5 ml/min and the liquid flow rate is 20 ml/h by using stainless steel mesh number 100. The results of the effect of channel thickness are shown in Figure 4.24 and it is found that the percent toluene removal efficiency is 96.1, 95.5 and 93.0 when the channel thickness

of gas and liquid are 250, 500 and 750 microns, respectively. The toluene removal efficiency by using 250 microns of channel thickness is higher than using channel thickness 500 and 750 microns due to decreasing of diffusion distance between toluene in the gas phase and vegetable oil.

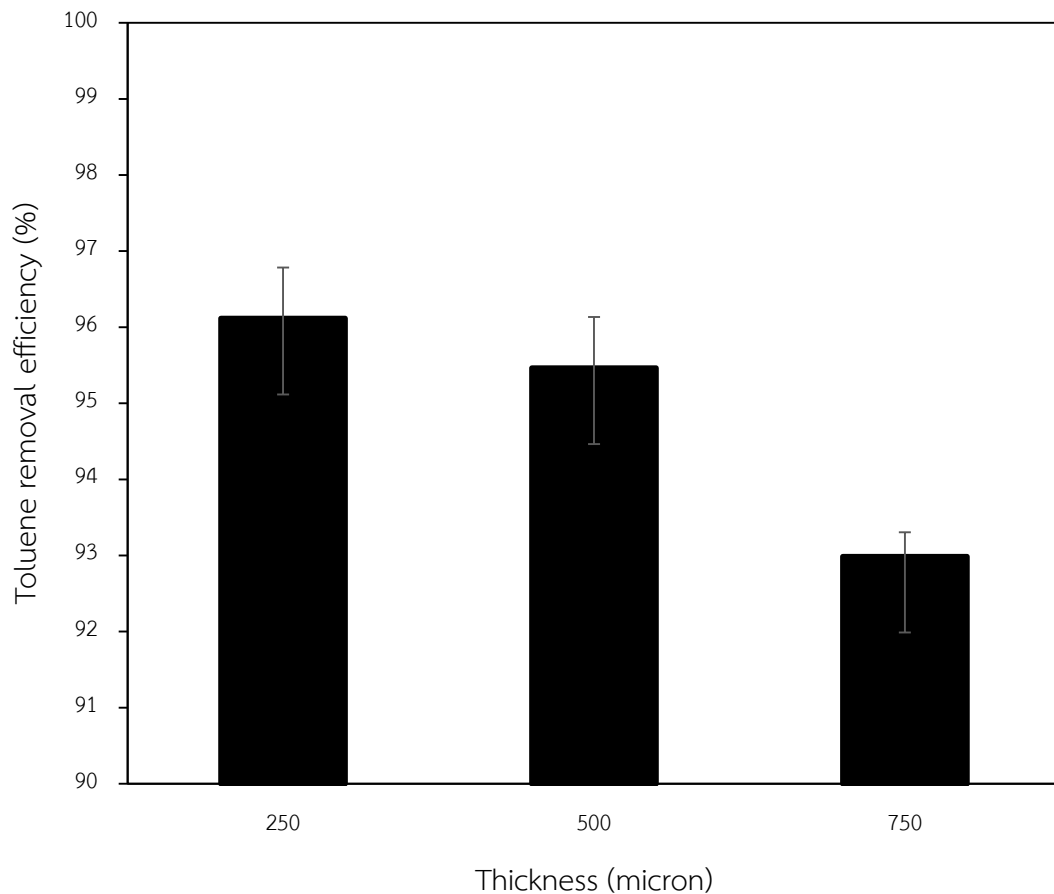


Figure 4.24 Effect of mesh size on toluene removal efficiency

When the thickness of channel is increased, the resident time of gas and liquid in the microchannel is also increased which can cause the increasing of contact time between gas and vegetable oil. The resident time of gas is 1.13, 2.25 and 3.38 when the channel thickness is 250, 500 and 750 microns, respectively. The toluene removal efficiency should increase when contact time is increased as described above. But the toluene removal efficiency decreases due to the decreasing of diffusion distance. The toluene in the gas phase is easily absorbed because the boundary layer thickness of

gas and liquid phase decreases with decreasing channel thickness, resulting in a decrease of the liquid phase resistance and the increase of the mass transfer. The liquid-side volumetric mass transfer coefficients are presented in Figure 4.25 and confirmed that the mass transfer of VOC in the gas phase in the liquid solvent is increased by decreasing channel thickness.

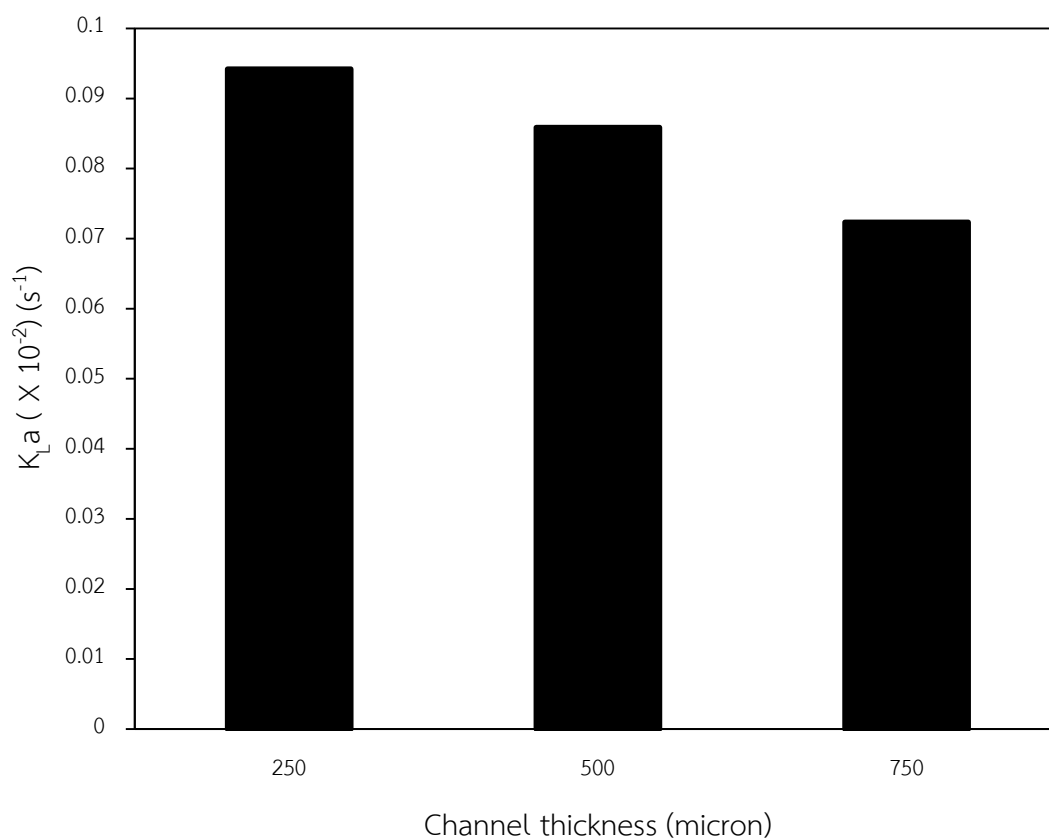


Figure 4.25 Effect of channel thickness the liquid-side volumetric mass transfer coefficients

Effect of inlet gas concentration

In order to observe the influence of the inlet gas concentration on toluene removal efficiency, the different inlet gas toluene concentration is prepared by controlling the different temperature of liquid toluene. The toluene gas concentration is varied as 11668, 17741 and 23338 ppm. The liquid and gas flow rate are kept constant at 20 ml/h and 5 ml/min, respectively. The effect of inlet gas toluene concentration on the toluene removal efficiency is shown in Figure 4.26. It shows that the percent of toluene removal efficiency is 92.1, 90.7 and 88.3 when of inlet gas toluene concentration is 11668, 17741 and 23338 ppm, respectively. The toluene removal efficiency decreases when inlet gas toluene concentration is increased because the increasing concentration of toluene in gas phase will allow more toluene molecules to travel from gas to the gas – liquid interface.

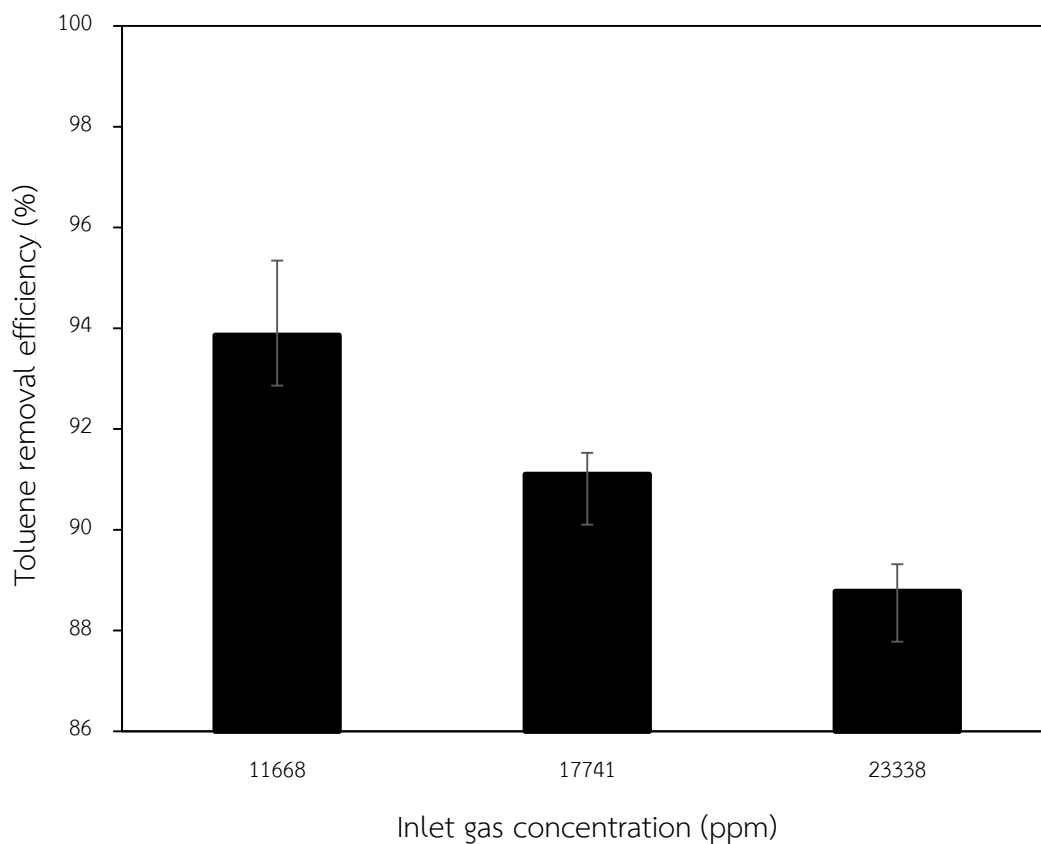


Figure 4.26 Effect of inlet gas concentration on the toluene removal efficiency

However, the absorption rate does not depend on the mass transfer of gas phase. So, the mass transfer in liquid phase plays a crucial role. For the absorption of VOC in the microchannel, the liquid phase mass transfer is considered to be a major factor which controls the absorption process system.

Figure 4.27 shows the liquid-side volumetric mass transfer coefficients which decreases with increasing of inlet gas concentration as same as the toluene removal efficiency.

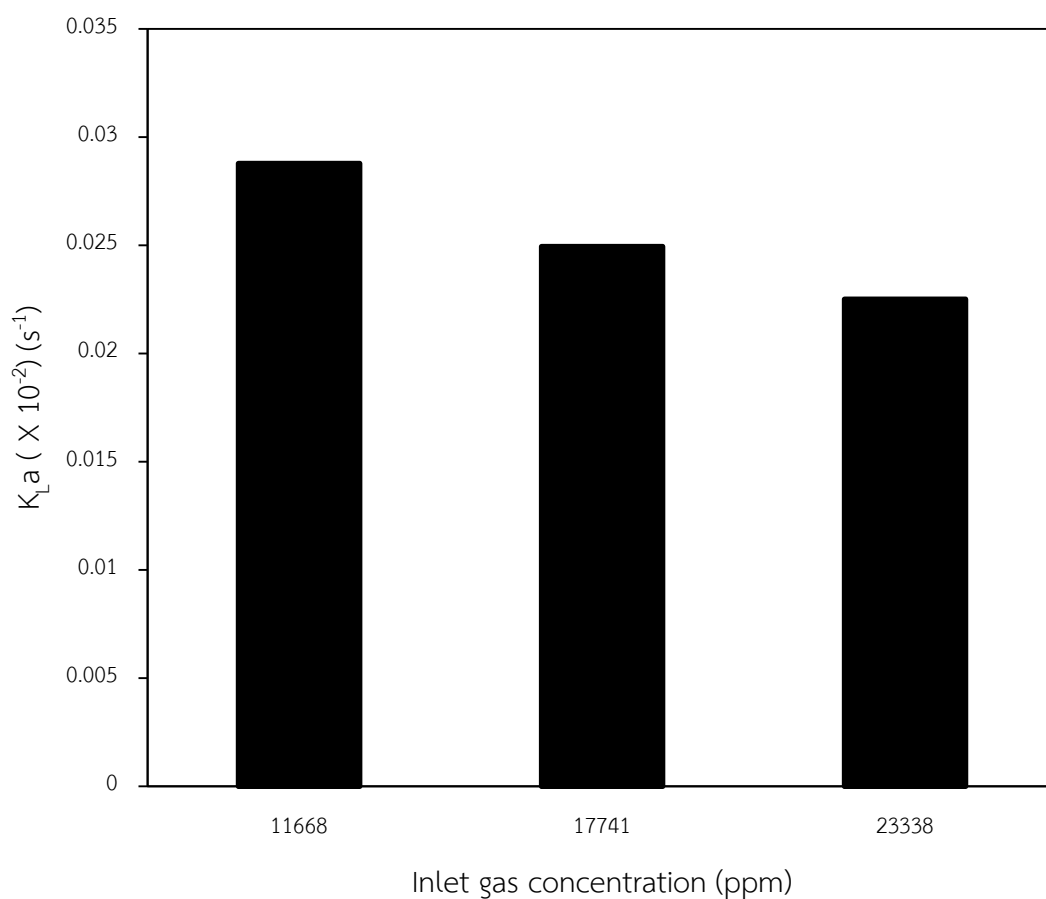


Figure 4.27 Effect of inlet gas concentration the liquid-side volumetric mass transfer coefficients

Effect of modified stainless steel mesh

In order to study the influence of the two different surface property of stainless steel mesh, one of stainless steel mesh is modified by coating the hydrophobic substance and another is unmodified which has a hydrophilic property. The gas flow rate in this experiment is 5 ml/min and the liquid flow rate is 20 ml/h by using stainless steel mesh number 100. The effect of two different surface property on the toluene removal efficiency is presented in Figure 4.28. The toluene removal efficiency is the same value when modified and unmodified stainless steel mesh is used. This can be considered that the influence of surface property of stainless steel mesh does not affect the VOC removal efficiency but it plays a crucial role in the flow pattern regime as described in part 4.2.

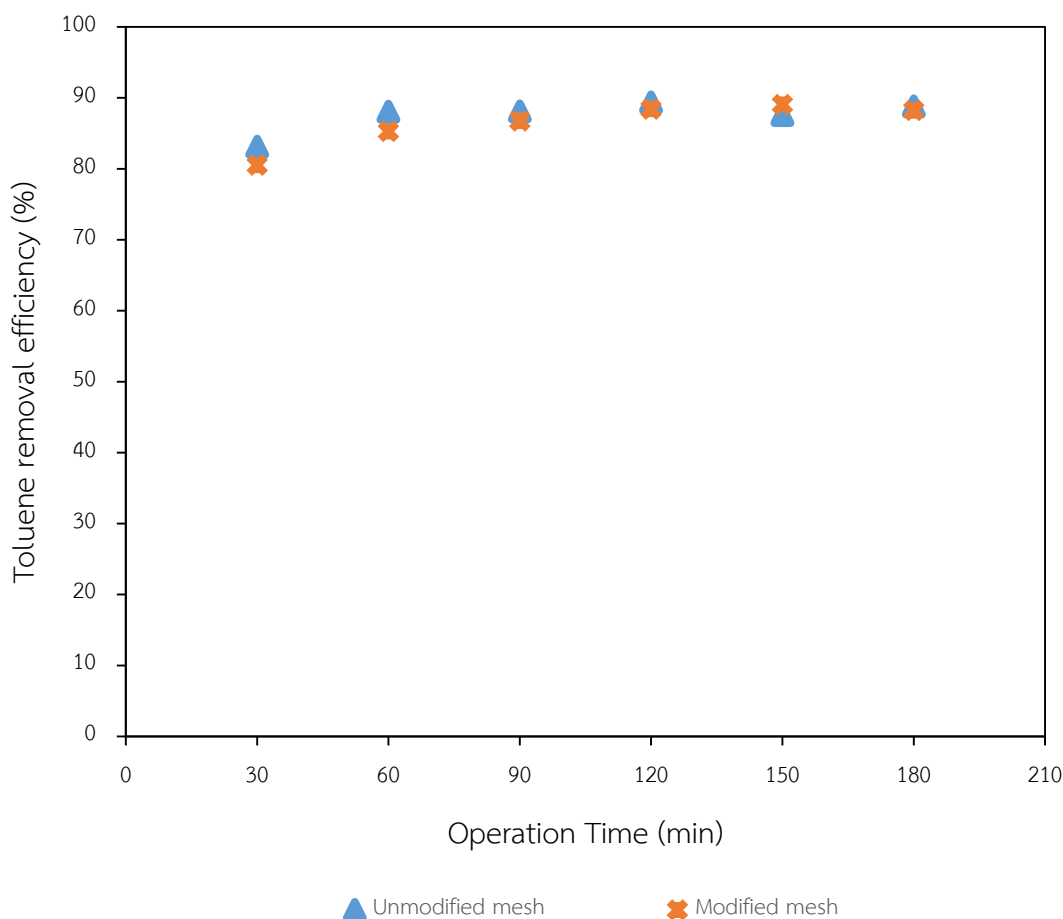


Figure 4.28 Effect of modified stainless steel mesh on the toluene removal efficiency

CHAPTER V

CONCLUSION

5.1 Summary of the results

5.1.1 Flow pattern regime of gas and liquid solvent by using stainless steel mesh in microchannel

1. The flow pattern regime can be classified into three types; gas and liquid solvent are completely separated, gas bubbles are detected in the outlet of liquid solvent, and liquid solvent is detected in the outlet of gas.

2. The gas to liquid solvent flow rate ratios are a factor to control separation of gas and the liquid solvent.

3. Mesh size plays a significant role in keeping gas and the liquid solvent separated. The smaller the pores, the higher the capillary force to hold the gas separates from the liquid.

4. The capillary force of liquid solvent within pores of mesh depends on a polarity of liquid solvent and mesh.

5. The flow pattern regime of hydrophobic stainless steel mesh regime which gas and vegetable oil are completely separated is wider than using stainless steel mesh. But the improving of flow pattern regime by modifying of stainless steel mesh is worse than using small stainless steel mesh size.

6. The pressure drop in microchannel is negligible and it is ensured that the flow pattern at each position in the microchannel is the same.

5.1.2 Absorption of volatile organic compound in a microchannel

1. Vegetable oil is a suitable liquid solvent for absorption process of volatile organic compound because it has high $1/H^*$ value, 1667, which assures that vegetable oil has high capacity of volatile organic compound absorption.

2. The flow pattern which gas and liquid solvent are incomplete separation lead to reducing of the interfacial area and decreasing of the removal efficiency.

3. The volatile organic compound removal efficiency is increased when liquid flow rate, channel length, mesh size and inlet gas concentration are increased.

4. The increasing of gas flow rate and channel thickness lead to decreasing of volatile organic compound removal efficiency.

5. The surface property of mesh does not affect the volatile organic compound removal efficiency.

6. The liquid-side volumetric mass transfer coefficient by using microchannel in this work was up to 0.00165 s^{-1} and it is higher than conventional absorbers.

5.2 Conclusion

The enhancement of volatile organic compound absorption process can be accomplished by using stainless steel mesh in microchannel. Vegetable oil is suitable model of liquid solvent for studying the volatile organic compound absorption process because it has high capacity of volatile organic compound absorption. The stainless steel mesh can allow gas and vegetable oil contact directly without dispersion of one phase into the other and it lead to increasing of interfacial area between gas and liquid solvent. The separation of gas and liquid solvent can be controlled by the gas to liquid solvent ratios. Besides, size and surface property of stainless steel mesh play a crucial role in keeping gas and the liquid solvent separated. In addition, the flow pattern at each position in the microchannel is the same because the pressure drop within microchannel is low. However, when gas disperses into liquid solvent to be a slug of gas, the interfacial area between gas and liquid solvent is decreased which leads to decreasing of volatile organic compound removal efficiency. The volatile organic compound removal efficiency also depends on the influence of gas flow rate, liquid flow rate, channel length, channel thickness, mesh size and inlet gas concentration.

Finally, the results of liquid-side volumetric mass transfer coefficient shows that using microchannel as an absorber can enhance the removal of volatile organic compound which cannot be achieved in conventional absorbers.



REFERENCES

1. Heymes, F., et al., *A new efficient absorption liquid to treat exhaust air loaded with toluene*. Chemical Engineering Journal, 2006. **115**(3): p. 225-231.
2. Xiang, Z., et al., *Absorption and desorption of gaseous toluene by an absorbent microcapsules column*. Journal of Hazardous Materials, 2010. **173**(1-3): p. 243-248.
3. Bay, K., H. Wanko, and J. Ulrich, *Absorption of Volatile Organic Compounds in Biodiesel*. Chemical Engineering Research and Design, 2006. **84**(1): p. 22-28.
4. Monnier, H., N. Mhiri, and L. Falk, *Falling liquid film stability in microgas/liquid absorption*. Chemical Engineering and Processing: Process Intensification, 2010. **49**(9): p. 953-957.
5. Khan, F.I. and A. Kr. Ghoshal, *Removal of Volatile Organic Compounds from polluted air*. Journal of Loss Prevention in the Process Industries, 2000. **13**(6): p. 527-545.
6. Hariz, R., et al., *Absorption of toluene by vegetable oil-water emulsion in scrubbing tower: Experiments and modeling*. Chemical Engineering Science, 2017. **157**: p. 264-271.
7. Li, R., et al., *Reduction of VOC emissions by a membrane-based gas absorption process*. Journal of Environmental Sciences, 2009. **21**(8): p. 1096-1102.
8. Rahbar, M.S. and T. Kaghazchi, *Modeling of packed absorption tower for volatile organic compounds emission control*. International Journal of Environmental Science & Technology, 2005. **2**(3): p. 207-215.
9. Treybal, R.E., *Mass-transfer operations*. 1981: McGraw-Hill Chemical Engineering Series.
10. Ozturk, B. and D. Yilmaz, *Absorptive Removal of Volatile Organic Compounds from Flue Gas Streams*. Process Safety and Environmental Protection, 2006. **84**(5): p. 391-398.

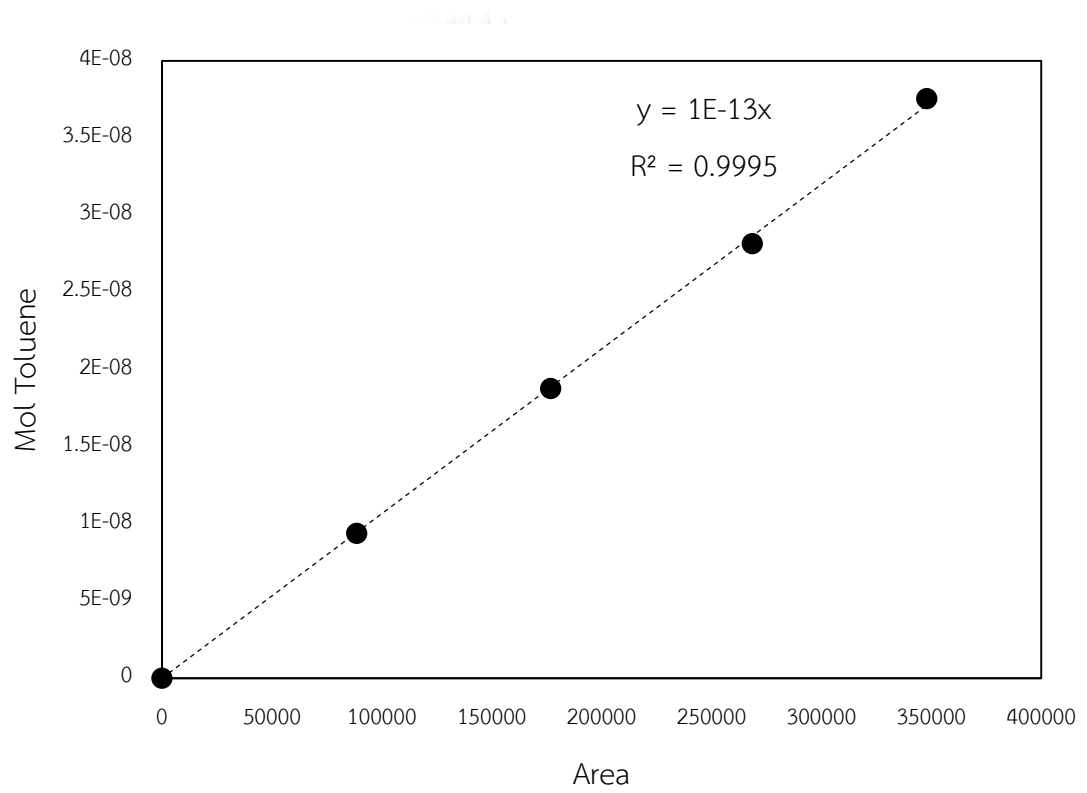
11. Prausnitz, J.M., R.N. Lichtenthaler, and E.G.d. Azevedo, *Molecular Thermodynamics of Fluid-Phase Equilibria*. 1999: Prentice-Hall.
12. J. Smith, H.V., M. Abbott, *Introduction to Chemical Engineering Thermodynamics*. 2005: McGraw-Hill.
13. Vuong, M.D., et al., *Determination of the Henry's constant and the mass transfer rate of VOCs in solvents*. Chemical Engineering Journal, 2009. **150**(2-3): p. 426-430.
14. Ye, C., et al., *Process analysis on CO₂ absorption by monoethanolamine solutions in microchannel reactors*. Chemical Engineering Journal, 2013. **225**: p. 120-127.
15. Ganapathy, H., et al., *Hydrodynamics and mass transfer performance of a microreactor for enhanced gas separation processes*. Chemical Engineering Journal, 2015. **266**: p. 258-270.
16. Constantinou, A., et al., *CO₂ absorption in a high efficiency silicon nitride mesh contactor*. Chemical Engineering Journal, 2012. **207-208**: p. 766-771.
17. Michalski, M.-C., et al., *Adhesion of edible oils to food contact surfaces*. Journal of the American Oil Chemists' Society, 1998. **75**(4): p. 447.
18. Bruus, H., *Theoretical microfluidics*. 2006: Department of Micro and Nanotechnology Technical University of Denmark.
19. Ganapathy, H., et al., *Fluid flow and mass transfer characteristics of enhanced CO₂ capture in a minichannel reactor*. Applied Energy, 2014. **119**: p. 43-56.
20. Pan, M.-Y., et al., *Selective absorption of H₂S from a gas mixture with CO₂ in a microporous tube-in-tube microchannel reactor*. Chemical Engineering and Processing: Process Intensification, 2015. **95**: p. 135-142.

APPENDIX

APPENDIX A

Calibration curve of toluene

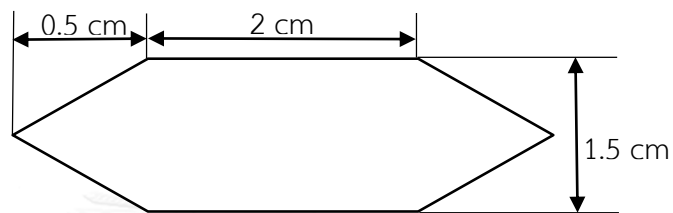
The calibration curve of toluene was analyzed by gas chromatography.



APPENDIX B

Calculation

Surface area and volume of channel



Thickness 250 micron

$$\begin{aligned}
 \text{Surface area of gas and liquid channel} &= (2 \times 1.5) + (2 \times \frac{1}{2} \times 0.5 \times 1.5) \\
 &= 3.75 \quad \text{cm}^2 \\
 &= 3.75 \times 10^{-4} \quad \text{m}^2 \\
 &= 0.5821 \quad \text{in}^2
 \end{aligned}$$

$$\begin{aligned}
 \text{Volume of gas and liquid channel} &= 3.75 \times 10^{-4} \times 250 \times 10^{-6} \\
 &= 9.375 \times 10^{-8} \quad \text{m}^3
 \end{aligned}$$

Contact area between gas and liquid solvent

Stainless steel mesh was placed between gas and liquid channel. So, gas and liquid solvent contact within square pores of stainless steel mesh.

Example

Stainless steel mesh number 100 has 100 pores in 1 inch and pore size 0.153 millimeters.

Extrapolation

If 1 square inch have 10^4 pores

So, 0.5821 square inch have 5821 pores

Contact area can be calculated from area of each pores multiply with amount of pore.

$$\begin{aligned} \text{Contact area between gas and liquid solvent (A)} &= 5821 \times 0.153 \times 0.153 \\ &= 136.27 \quad \text{mm}^2 \\ &= 136.27 \times 10^{-6} \quad \text{m}^2 \end{aligned}$$

Specific interfacial area

Specific interfacial area is defined as the ratio of contact area between gas and liquid solvent and volume of microchannel as show in equation 1b.

$$a = \frac{A}{V} \quad (1b)$$

where a specific interfacial area (m^{-1})
 A contact area between gas and liquid solvent (m^2)
 V volume of microchannel (m^3)

Example

For stainless steel mesh number 100,

$$a = \frac{136.27 \times 10^{-6}}{2 \times 9.375 \times 10^{-8}}$$

$$a = 726.78 \text{ m}^{-1}$$

Residence time

Residence time can be calculated as equation 2a.

$$t = \frac{V}{Q} \quad (2b)$$

where V volume of microchannel (m^3)
 Q gas or liquid flow rate (m^3/s)

Example

For liquid flow rate 20 ml/h,

$$t = \frac{9.375 \times 10^{-10} \text{ m}^3}{20 \text{ ml/h}} \times \frac{1000 \text{ ml}}{1 \text{ l}} \times \frac{1000 \text{ l}}{1 \text{ m}^3} \times \frac{3600 \text{ sec}}{1 \text{ h}}$$

$$t = 16.77 \text{ sec}$$

Concentration of toluene in gas and liquid solvent

The concentration of toluene in gas phase can be calculated from peak area of gas chromatography by using calibration curve. From the experiment, we can find equation of calibration curve as following equation:

$$y = 10^{-13} x \quad (3b)$$

where y mol of toluene (mol)

x peak area of gas chromatography

Example

The result of inlet concentration of toluene in gas phase from gas chromatography shows peak area and retention time by using injection volume 0.2 ml.

Toluene in gas phase	
Retention time (min)	peak area
1.8	1958018

$$\text{Mol of toluene} = 1958018 \times 10^{-13} \text{ mol}$$

$$\text{Concentration of toluene} = \frac{\text{Mol of toluene}}{\text{Injection volume}}$$

$$= \frac{1958018 \times 10^{-13} \text{ mol}}{0.2 \times 10^{-3} \text{ l}}$$

$$= 9.79 \times 10^{-4} \text{ mol/l}$$

The concentration of toluene in liquid phase can be calculated from mass balance as equation 4b.

$$C_{L,out} = \frac{Q_G(C_{G,in} - C_{G,out})}{Q_L} + C_{L,in} \quad (4b)$$

where $C_{L,out}$ outlet liquid concentration (mol/l)
 $C_{L,in}$ inlet liquid concentration (mol/l)
 Q_L liquid flow rate (m³/s)
 Q_G gas flow rate (m³/s)
 $C_{G,in}$ inlet gas concentration (mol/l)
 $C_{G,out}$ outlet gas concentration (mol/l)

Example

The concentration of toluene in liquid phase when gas flow rate, liquid flow rate, inlet gas concentration, outlet gas concentration and inlet liquid concentration are 5ml/min, 20ml/h, 9.79×10^{-4} mol/l, 2.93×10^{-5} mol/l and 0 mol/l, respectively.

$$C_{L,out} = \left(\frac{5 \text{ ml/min} \times (9.79 \times 10^{-4} \text{ mol/l} - 2.93 \times 10^{-5})}{20 \text{ ml/h}} \times \frac{60 \text{ min}}{1 \text{ h}} \right) + 0$$

$$= 0.0142 \text{ mol/l}$$

Toluene removal efficiency

The toluene removal efficiency can be estimated by following equation:

$$X = \left(1 - \frac{C_{G,out}}{C_{G,in}} \right) \times 100\% \quad (5b)$$

where X = toluene removal efficiency (%)

Example

The toluene removal efficiency when inlet gas concentration and outlet gas concentration are 9.79×10^{-4} mol/l and 2.93×10^{-5} mol/l.

$$X = \left(1 - \frac{2.93 \times 10^{-5}}{9.79 \times 10^{-4}} \right) \times 100\%$$

$$X = 97.01 \%$$

Equilibrium inlet and outlet concentration of liquid solvent

The equilibrium inlet and outlet concentration of liquid solvent can be calculated from Henry's law constant. From the experiment, the relative of equilibrium gas concentration and equilibrium liquid concentration can be expressed by following equation:

$$C_{i,G} = 0.0006C_{i,L} \quad (6b)$$

where $C_{i,G}$ = equilibrium gas concentration (mol/l)

$C_{i,L}$ = equilibrium liquid concentration (mol/l)

Example

The equilibrium inlet and outlet concentration of liquid solvent in counter-flow absorber when inlet gas concentration and outlet gas concentration are 9.79×10^{-4} mol/l and 2.93×10^{-5} mol/l.

$$\begin{aligned} \text{equilibrium inlet concentration of liquid solvent} &= \frac{2.93 \times 10^{-5}}{0.0006} \\ &= 0.049 \text{ mol/l} \end{aligned}$$

and

$$\begin{aligned} \text{equilibrium outlet concentration of liquid solvent} &= \frac{9.79 \times 10^{-4}}{0.0006} \\ &= 1.63 \text{ mol/l} \end{aligned}$$

Mass transfer coefficient

The volumetric mass transfer coefficient based on the liquid phase in counter-flow absorber can be determined by equation 7b. and 8b.

$$k_L a = \frac{Q_L (C_{L,out} - C_{L,in})}{V \Delta C_M} \quad (7b)$$

$$\Delta C_M = \frac{(C_{i,in} - C_{L,in}) - (C_{i,out} - C_{L,out})}{\ln((C_{i,in} - C_{L,in}) / (C_{i,out} - C_{L,out}))} \quad (8b)$$

where $k_L a$ volumetric mass transfer coefficient (s^{-1})

ΔC_M log mean concentration of liquid solvent (mol/l)

$C_{i,in}$ equilibrium inlet concentration of liquid solvent (mol/l)

$C_{i,out}$ equilibrium outlet concentration of liquid solvent (mol/l)

Example

The volumetric mass transfer coefficient when gas flow rate, inlet gas concentration, outlet gas concentration, inlet liquid concentration, and outlet liquid concentration are 20 ml/h, 9.79×10^{-4} mol/l, 2.93×10^{-5} mol/l, 0 mol/l and 0.0142 mol/l, respectively.

$$\Delta C_M = \frac{(0.049 - 0) - (1.63 - 0.0142)}{\ln((0.049 - 0)/(1.63 - 0.0142))}$$

$$= 0.448 \text{ mol/l}$$

$$k_L a = \frac{20 \text{ ml/h} \times (0.0142 - 0) \text{ mol/l}}{1.875 \times 10^{-7} \text{ m}^3 \times 0.448 \text{ mol/l}} \times \frac{1 \text{ l}}{1000 \text{ ml}} \times \frac{1 \text{ m}^3}{1000 \text{ l}} \times \frac{1 \text{ h}}{3600 \text{ sec}}$$

$$= 9.39 \times 10^{-4} \text{ s}^{-1}$$

Pressure drop

Pressure drop in rectangular microchannel can be determined by H. Bruus with following equation

$$\Delta P = \frac{12\mu L Q}{h^3 W} \frac{1}{1-0.630(h/W)} \quad (9b)$$

where ΔP pressure drop ($\text{kg/s}^2\text{m}$, Pa)

μ viscosity (kg/s.m , Pa.s)

L length (m)

W width (m)

h height (m)

Q fluid flow rate (m^3/s)

Example

Pressure drop within liquid channel when using vegetable oil which has viscosity 0.057 Pa.s and flow rate 20 ml/h

$\Delta P =$

$$\frac{12 \times 0.057 \text{ kg/s.m} \times 0.02 \text{ m} \times 20 \text{ ml/h}}{\frac{(250 \times 10^{-6} \text{ m})^3 \times 0.015 \text{ m}}{1 \text{ m}^3} \times \frac{1 \text{ h}}{3600 \text{ sec}}} \times \frac{1}{1 - 0.630(250 \times 10^{-6} \text{ m}/0.015 \text{ m})} \times \frac{1 \text{ l}}{1000 \text{ ml}} \times$$

$$= 327.71 \text{ Pa}$$

$$= 0.328 \text{ kPa}$$

Pressure drop within gas channel when air has viscosity 0.0000181 Pa.s and flow rate 5 ml/min

$\Delta P =$

$$\frac{12 \times 1.81 \times 10^{-5} \text{ kg/s.m} \times 0.02 \text{ m} \times 5 \text{ ml/min}}{\frac{(250 \times 10^{-6} \text{ m})^3 \times 0.015 \text{ m}}{1 \text{ m}^3} \times \frac{1 \text{ h}}{60 \text{ min}}} \times \frac{1}{1 - 0.630(250 \times 10^{-6} \text{ m}/0.015 \text{ m})} \times \frac{1 \text{ l}}{1000 \text{ ml}} \times$$

$$= 1.56 \text{ Pa}$$

$$= 0.00156 \text{ kPa}$$

Surface tension in capillary tube

Surface tension in capillary tube can be determined by Young – Laplace equation with following equation:

$$\gamma = \frac{\rho g r H}{2 \cos \theta} \quad (10b)$$

where γ Surface tension (N/m)
 ρ density of liquid (kg/m³)
 g gravitational acceleration (m/s²)
 r radius of capillary tube (m)
 H height of liquid in capillary tube (m)
 θ contact angle (degree)

Example

The surface tension of vegetable oil in glass capillary tube which has radius 0.9 mm when density of vegetable oil, contact angle and height of vegetable oil in capillary tube are 918.25 kg/m³, 28° and 0.006 m, respectively.

$$\begin{aligned} \gamma &= \frac{918.25 \text{ kg/m}^3 \times 9.8 \text{ m/s}^2 \times 0.0009 \text{ m} \times 0.006 \text{ m}}{2 \cos(28^\circ)} \\ &= 0.028 \text{ N/m} \end{aligned}$$

Capillary pressure in capillary tube

Capillary pressure in capillary tube can be determined by Young – Laplace equation with following equation:

$$\Delta P = \frac{2\gamma \cos \theta}{r} \quad (11b)$$

Example

Capillary pressure of vegetable oil in glass capillary tube which has radius 0.9 mm when surface tension of vegetable oil and contact angle are 0.028 N/m and 28°.

$$\begin{aligned}\Delta P &= \frac{2 \times 0.028 \text{ N/m} \times \cos(28^\circ)}{0.0009 \text{ m}} \\ &= 54 \text{ N/m}^2\end{aligned}$$

Minimum liquid-gas ratio for counter-current flow absorber

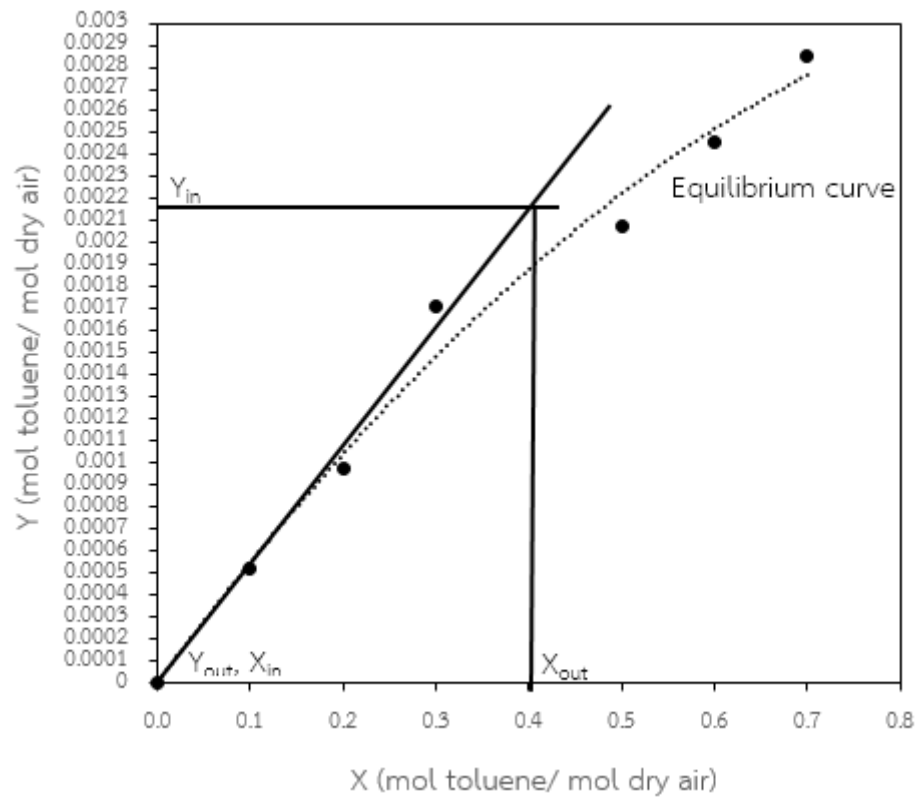
The Minimum liquid-gas ratio is calculated at 97% removal efficiency. Gas flow rate is 5 ml/min containing 0.000960 mol/l of toluene. The pure vegetable oil (sunflower oil) is fed at 40 ml/h.

$$\begin{aligned}Y_{in} &= \frac{0.00960 \text{ mol toluene}}{1 \text{ L dry air}} \times \frac{1 \text{ L}}{1000 \text{ ml}} \times \frac{1 \text{ ml}}{0.0128 \text{ g dry air}} \times \frac{28.97 \text{ g dry air}}{1 \text{ mol dry air}} \\ &= 2.17 \times 10^{-3} \text{ mol toluene/mol dry air}\end{aligned}$$

$$\begin{aligned}Y_{out} &= (0.03)(2.17 \times 10^{-3}) \\ &= 6.52 \times 10^{-3} \text{ mol toluene/mol dry air}\end{aligned}$$

$$X_{in} = 0 \text{ mol toluene/mol dry air}$$

The composition of the outlet liquid solvent (X_{out}) can acquire from equilibrium-curve of toluene and vegetable oil.



$$X_{in} = 0.4 \text{ mol toluene/mol dry air}$$

$$\begin{aligned} (L/G)_{min} &= \frac{Y_{in} - Y_{out}}{X_{out} - X_{in}} \\ &= 5.26 \times 10^{-3} \text{ mol vegetable oil/mol dry air} \end{aligned}$$

VITA

Mr. Rachata Prasomsup was born on April 24, 1993 in Nakhonratchasima, Thailand. In 2015, he graduated from Chemical Technology, Chulalongkorn University in Bachelor of Science (Chemical Engineering). After that, he joined the Department of Chemical Engineering, Chulalongkorn University, as a master's degree student. In 2017, he graduated with a thesis entitled "Use of metal mesh to increase absorption efficiency of volatile organic compound in microchannel"

